

LABORATORY DETERMINATION OF ROCK MASS ELASTIC
MODULUS USING ULTRASONIC PULSE VELOCITY



KRITTIYAPORN SINGKRAIHAN

A Thesis Submitted in Partial Fulfillment of the Requirement for the
Degree of Master of Philosophy of Engineering in Civil, Transportation
and Geo-Resources Engineering
Suranaree University of Technology
Academic Year 2021

การวัดความยืดหยุ่นของมวลหินในห้องปฏิบัติการโดยใช้คลื่นอัลตราโซนิก




วิทยานิพนธ์นี้เป็นส่วนหนึ่งของการศึกษาตามหลักสูตรปริญญาวิศวกรรมศาสตรมหาบัณฑิต
สาขาวิชาวิศวกรรมโยธา ขนส่ง และทรัพยากรธรณี
มหาวิทยาลัยเทคโนโลยีสุรนารี
ปีการศึกษา 2564


LABORATORY DETERMINATION OF ROCK MASS ELASTIC MODULUS
USING ULTRASONIC PULSE VELOCITY

Suranaree University of Technology has approved this thesis submitted in partial fulfillment of the requirements for a Master's Degree.


Thesis Examining Committee



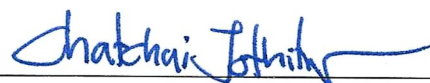
(Assoc. Prof. Dr. Pornkasem Jongpradish)
Chairperson



(Prof. Dr. Kittitep Fuenkajorn)
Member (Thesis Advisor)



(Asst. Prof. Dr. Prachya Tepnarong)
Member



(Assoc. Prof. Dr. Chatchai Jothityangkoon)
Vice Rector for Academic Affairs
and Quality Assurance



(Assoc. Prof. Dr. Pornsiri Jongkol)
Dean of Institute of Engineering

กฤติยาพร สิงห์ไกรหาญ : การวัดความยืดหยุ่นของมวลหินในห้องปฏิบัติการโดยใช้คลื่น
อัลตราโซนิก (LABORATORY DETERMINATION OF ROCK MASS ELASTIC MODULUS
USING ULTRASONIC PULSE VELOCITY) อาจารย์ที่ปรึกษา : ศาสตราจารย์ ดร.กิตติเทพ
เฟื่องขจร, 74 หน้า.

คำสำคัญ: สัมประสิทธิ์ของความยืดหยุ่น/ความเร็วคลื่น/รอยแตกของหิน/สัมประสิทธิ์การยุบตัวใน
แนวตั้งฉาก/รอยแตกจำลอง

วัตถุประสงค์ของการศึกษานี้เพื่อหาคุณสมบัติความยืดหยุ่นของแบบจำลองมวลหินผ่าน
การทดสอบเชิงพลศาสตร์และเปรียบเทียบกับผลลัพธ์จากการทดสอบเชิงสถิต โดยได้สร้าง
ความสัมพันธ์ระหว่างสัมประสิทธิ์ของความยืดหยุ่นเชิงพลศาสตร์และเชิงสถิตของหิน 9 ชนิด
การศึกษานี้แนะนำแนวทางการใช้ความเร็วของคลื่นเพื่อกำหนดคุณสมบัติความยืดหยุ่นของหิน
ในห้องปฏิบัติการภายใต้สภาวะแห้งของแท่งตัวอย่างหินที่มีการจำลองรอยแตกจำนวน 1-5 รอยแตก
(รอยแตกที่เกิดจากแรงดึง) การยุบตัวของรอยแตกในแนวตั้งฉากถูกตรวจวัดและหาความสัมพันธ์
ระหว่างคุณสมบัติยืดหยุ่นเชิงพลศาสตร์และเชิงสถิต ซึ่งความเร็วคลื่น สัมประสิทธิ์ของความยืดหยุ่น
เชิงพลศาสตร์และเชิงสถิตมีค่าลดลงเมื่อมีการเพิ่มขึ้นของจำนวนรอยแตก สัมประสิทธิ์ของ
ความยืดหยุ่นเชิงพลศาสตร์ของหินที่ไม่มีรอยแตกมีค่าเป็นสองเท่าของความยืดหยุ่นเชิงสถิต และ
พบความสัมพันธ์ที่ระหว่างสัมประสิทธิ์ความยืดหยุ่นเชิงพลศาสตร์และเชิงสถิตของแบบจำลอง
มวลหินโดยใช้สมการพหุนาม

สาขาวิชา เทคโนโลยีธรณี
ปีการศึกษา 2564

ลายมือชื่อนักศึกษา กฤติยาพร สิงห์ไกรหาญ
ลายมือชื่ออาจารย์ที่ปรึกษา ศ.กิตติเทพ

KRITTIYAPORN SINGKRAIHAN : LABORATORY DETERMINATION OF ROCK MASS ELASTIC MODULUS USING ULTRASONIC PULSE VELOCITY. THESIS ADVISOR : PROF. KITTITEP FUENKAJORN, Ph.D., 74 PP.

Keyword: Young's modulus/Wave velocity/Rock fractures/Joint normal stiffness/
Artificial fracture

The objective of this study is to determine elastic properties of rock mass models through dynamic testing and compare them with the results from static testing. Correlation is made between the dynamic Young's modulus and static Young's modulus of nine rock types. This study presents approaches to use waves velocities for the laboratory determination of rock elastic properties under dry condition of rock core specimens with one to five artificial fractures (tension-induced fractures). Joint normal stiffness is measured and incorporated into the relationship between the dynamic and static properties of the specimens. It is found that the wave velocities, static, and dynamic Young's moduli decrease with increasing number of fractures. The dynamic Young's modulus for intact rocks is about twice of their static Young's modulus. Good correlation is obtained between dynamic and static Young's moduli of the rock mass models via polynomial equations.

มหาวิทยาลัยเทคโนโลยีสุรนารี

School of Geotechnology
Academic year 2021

Student's Signature กฤติยาพร สิงครไหาน
Advisor's Signature Le. Kittitep

ACKNOWLEDGEMENTS

I wish to acknowledge the funding support from Suranaree University of Technology (SUT).

I would like to express my deepest thanks to Prof. Dr. Kittitep Fuenkajorn, thesis advisor, who gave a critical review. Furthermore, I appreciate the encouragement, suggestions, and comments during the research period. I would like to express my sincere thanks to Assoc. Prof. Dr. Pornkasem Jongpradist, and Asst. Prof. Dr. Prachya Tepnarong for their valuable suggestions and comments on my research works as thesis committee members. Thanks are given to all staffs of the Geomechanics Research Unit, Institute of Engineering who supported my work.

Finally, I most appreciatively acknowledge my parents, and my friends for all their supported throughout the period of this study.

Krittiyaporn Singkraihaan



มหาวิทยาลัยเทคโนโลยีสุรนารี

TABLE OF CONTENTS

	Page
ABSTRACT (THAI).....	I
ABSTRACT (ENGLISH).....	II
ACKNOWLEDGEMENTS	III
TABLE OF CONTENTS.....	IV
LIST OF TABLES.....	VI
LIST OF FIGURES	VII
SYMBOLS AND ABBREVIATIONS.....	XI
CHAPTER	
I INTRODUCTION	1
1.1 Background and rationale.....	1
1.2 Research objectives.....	1
1.3 Scope and limitations.....	1
1.4 Research methodology.....	2
1.4.1 Literature review.....	3
1.4.2 Sample preparation.....	3
1.4.3 Static loading.....	3
1.4.4 Pulse velocity test on roughness fracture.....	3
1.4.5 Mathematical Relationships.....	3
1.4.6 Discussions and Conclusions.....	3
1.4.7 Thesis Writing.....	3
1.5 Thesis content.....	4
II LITERATURE REVIEW.....	5
2.1 Introduction	5
2.2 Ultrasonic pulse velocity test	5
2.3 Effect of fracture on wave velocity.....	6
2.4 Effect of physical properties on wave velocity	14
2.5 Effect of mechanical properties on wave velocity.....	17
2.6 Deformations modulus and joint normal stiffness on rock mass.....	20
III SAMPLE PREPARATION.....	25
3.1 Introduction	25

TABLE OF CONTENTS (Continued)

	Page
3.2 Rock sample	25
3.3 Sample preparation.....	30
IV LABORATORY TESTING	32
4.1 Introduction	32
4.2 Static loading	32
4.3 Ultrasonic pulse velocity measurement.....	35
V TEST RESULTS	38
5.1 Introduction	38
5.2 Static loading tests	38
5.3 Ultrasonic pulse velocity (UPV) measurement tests.....	52
VI RELATIONSHIP BETWEEN STATIC AND DYNAMIC PARAMETER.....	56
6.1 Introduction	56
6.2 Dynamic deformation modulus.....	56
6.3 Static deformation modulus.....	57
6.4 Relationship of slope values of polynomial equation.....	59
6.5 Correlations between dynamic and static deformation moduli.....	61
6.6 Comparison with previous studies between dynamic and static deformation modulus.....	67
VII DISCUSSIONS AND CONCLUSIONS.....	68
7.1 Discussions	68
7.2 Conclusions.....	69
7.3 Recommendations for future studies.....	69
REFERENCES	70
BIOGRAPHY	74

LIST OF TABLES

Table		Page
1.1	Groups and type of rock samples that are test.....	2
2.1	Fracture surface pattern model	7
2.2	P-wave velocity tests result	7
2.3	Regression equations for each rock types.....	8
2.4	Results of V_p measurement on samples	11
2.5	P-wave VRR% in different joint numbers	13
2.6	Physical properties of calcarenite rocks	15
2.7	Regression analysis results.....	18
2.8	Parameter N defined for modified equation by Thaweeboon et al. (2017).	20
2.9	Linear relationship between static (E_{stat}) and dynamic (E_{dyn}) modulus ($E_{stat} = a \cdot E_{dyn} - b$) by Davarpanah et al. (2020).	23
3.1	Rock samples used for this study	25
3.2	Mineral compositions of rock specimens.....	26
3.3	Summary of physical properties of rock specimens.....	31
4.1	Strength and maximum applied axial stress of each rock types	34
4.2	Density for each rock type and after change of fractures are induced	37
5.1	Summary of physical and mechanical properties of rock specimens measured under static loading.....	48
5.2	Summary of physical properties of rock specimens for UPV measurements	53
6.1	Parameters of polynomial equation for dynamic deformation modulus of each rock type.....	57
6.2	Parameters of polynomial equation for static deformation modulus of each rock type.....	58
6.3	Parameters for prediction static deformation modulus depending on rock type	63

LIST OF FIGURES

Figure		Page
1.1	Research methodology	2
2.1	Graphic model of wave velocity measuring equipment (the PUN- DIT).....	6
2.2	Results of granite between P-wave velocity and FRC	8
2.3	Results of marble between P-wave velocity and FRC	9
2.4	Results of travertine between P-wave velocity and FRC.....	9
2.5	V_p measurement on samples in laboratory.....	10
2.6	Increasing fractures with different spacing	11
2.7	P-wave velocity with different fracture spacings	12
2.8	Average of VRR% compare increasing of fracture number with different spacing in Andesite rock samples	13
2.9	P-wave velocity compared porosity of dry samples	15
2.10	P-wave velocity compared with porosity of saturated samples	16
2.11	P-wave velocity compared with density of dry samples.....	16
2.12	P-wave velocity compared with density of dry samples.....	17
2.13	Correlation of wave velocity and UCS.....	18
2.14	Correlation of wave velocity and Young's modulus	18
2.15	Correlation of wave velocity and density	19
2.16	Relative result between P-wave velocity and UCS of rocks	19
2.17	Relationship between static E_s and dynamic E_d moduli for 5 different crystalline rock types.....	21
2.18	Calibration plotting show variation of Young's Modulus with joint normal stiffness of the particles	22
2.19	Calibration plotting show the variation of Peak Uniaxial Strength with joint normal stiffness of the particles	23
2.20	Plot of relationship between measured static and dynamic modulus of elasticity: $E_{stat} = a \cdot E_{dyn} - b$	24

LIST OF FIGURES (Continued)

Figure	Page
3.1 Representative laser scanned images of rough fracture for Phra Wihan sandstone (a), Sao Khua sandstone (b), Phu Tok sandstone (c), Phu Phan sandstone (d), Phu Kradung sandstone (e), Khao Khad marble (f), Khao Khad limestone (g), Khao Khad travertine (h), and Tak granite (i).	29
3.2 Cylindrical specimens before fracture is induced. Phra Wihan sandstone (a), Sao Khua sandstone (b), Phu Tok sandstone (c), Phu Phan sandstone (d), Phu Kradung sandstone (e), Khao Khad marble (f), Khao Khad limestone (g), Khao Khad travertine (h), and Tak granite (i).	30
4.1 Methodology of laboratory testing.....	32
4.2 Uniaxial compression test device	33
4.3 Creating an artificial fracture	34
4.4 Core specimens after all fractures is induced Phra Wihan sandstone (a), Sao Khua sandstone (b), Phu Tok sandstone (c), Phu Phan sandstone (d), Phu Kradung sandstone (e), Khao Khad marble (f), Khao Khad limestone (g), Khao Khad travertine (h), and Tak granite (i).	35
5.1 Static loading test results of each fracture for Phra Wihan sandstone	39
5.2 Static loading test results of each fracture for Sao Khua sandstone	40
5.3 Static loading tests result of each fracture for Phu Tok sandstone	41
5.4 Static loading test results of each fracture for Phu Phan sandstone.....	42
5.5 Static loading test results of each fracture for Phu Kradung sandstone	43
5.6 Static loading tests result of each fracture for Khao Khad marble.....	44
5.7 Static loading test results of each fracture for Khao Khad limestone	45
5.8 Static loading test results of each fracture for Khao Khad travertine	46
5.9 Static loading test results of each fracture for Tak granite.....	47
5.10 Relationship between change of fracture aperture (Δe) and number of fractures	50

LIST OF FIGURES (Continued)

Figure	Page
5.11 Relationship between joint normal stiffness (K_n) and number of fractures.....	50
5.12 Relationship between Young's moduli of fractured rock: $E_{m,m}$ and number of fractures.....	51
5.13 Relationship between Young's moduli of fractured rock: $E_{m,c}$ and number of fractures.....	51
5.14 Relationship between Young's moduli of fractured rock: $E_{m,m}$ and Young's moduli of fractured rock: $E_{m,c}$	52
5.15 Relationship between P-wave velocity (km/s) and number of fractures.....	55
5.16 Relationship between S-wave velocity (km/s) and number of fractures.....	55
6.1 Relationship between dynamic deformation modulus (E_d) and number of fractures.....	57
6.2 Relationship between static deformation modulus (E_s) and number of fractures.....	58
6.3 Slopes B (dynamic deformation modulus) and D (static deformation modulus) as a function of joint normal stiffness (K_n).	60
6.4 Relationship between slope B (Dynamic deformation modulus, E_d) and D (Static deformation modulus, E_s).....	60
6.5 Relationship between dynamic and static deformation moduli of Phra Wihan sandstone	62
6.6 Relationship between dynamic and static deformation moduli of Sao Khua sandstone.....	62
6.7 Relationship between dynamic and static deformation moduli of Phu Tok sandstone	63
6.8 Relationship between dynamic and static deformation moduli of Phu Phan sandstone.....	63
6.9 Relationship between dynamic and static deformation moduli of Kradung sandstone.....	64

LIST OF FIGURES (Continued)

Figure		Page
6.10	Relationship between dynamic and static deformation moduli of Khao Khad marble.....	64
6.11	Relationship between dynamic and static deformation moduli of Khao Khad limestone	65
6.12	Relationship between dynamic and static deformation moduli of Khao Khad travertine.....	65
6.13	Relationship between dynamic and static deformation moduli of Tak granite	66
6.14	Correlation between dynamic and static deformation modulus for all rock types.....	66
6.15	Comparison with previous studied between dynamic and static deformation; ① Belikov et al. (1970), ② King (1983), ③ Eissa and Kazi (1988), ④ McCann and Entwisle (1992), ⑤ Eissa and Kazi (1988), ⑥ Charitaras et al. (1994), ⑦ Nur and Wang (1999), ⑧ Brotons et al. (2014), and ⑨ Brotons et al. (2016).....	67

SYMBOLS AND ABBREVIATIONS

Δe	=	Changed of fracture aperture
A	=	Cross-sectional area of rock sample
B	=	Empirical constant for equation (6.1)
C	=	Empirical constant for equation (6.1)
D	=	Empirical constant for equation (6.2)
E_d	=	Dynamic Young's modulus
$E_{d,i}$	=	Dynamic modulus of intact rock
E_i	=	Intact rock deformation modulus
E_m	=	Jointed rock deformation modulus
$E_{m,c}$	=	Calculated Young's modulus of rock specimen
$E_{m,m}$	=	Measured Young's modulus of rock specimen
E_n	=	Equivalent deformation modulus
E_r	=	Rock deformation modulus
E_s	=	Static Young's modulus
$E_{s,i}$	=	Static modulus of intact rock
F	=	Empirical constant for equation (6.2)
K_n	=	Joint normal stiffness
L	=	Length of rock sample
N	=	Number of fractures
s	=	Average joint spacing
V_p	=	P-wave velocity
V_s	=	S-wave velocity
W	=	Weight of rock sample
X	=	Empirical constant for equation (6.6)
Y	=	Empirical constant for equation (6.6)
ν_d	=	Dynamic Poisson's ratio
$\sigma_{10\%}$	=	Selected maximum stress at 10%
ρ	=	Density of specimen

CHAPTER I

INTRODUCTION

1.1 Background and rationale

Deformation modulus of rock mass is an important parameter for geological engineering works. It dictates the settlement of foundations of buildings, dams, and bridges. Closure or convergence of mine opening and tunnel after excavation is also controlled by the rock mass deformability. Obtaining this parameter in the field (such as plate bearing test) can be time-consuming and expensive. Correlation between the Young's modulus of rock mass and that of the intact rock and joint stiffness is desirable. Such approach would allow predicting the rock mass modulus by using the calibrated stiffness properties of intact rock and joint properties.

1.2 Research objectives

The objective of this study is to determine the deformation modulus of rock mass model by using ultrasonic pulse velocity (UPV) measurement. The tasks involve ultrasonic pulse velocity measurements, determination of elastic modulus of intact core specimens, and with artificial fractures, and correlation between the dynamic Young's modulus and static Young's modulus of specimens.

1.3 Scope and limitations

The scope and limitations of this research include as follows

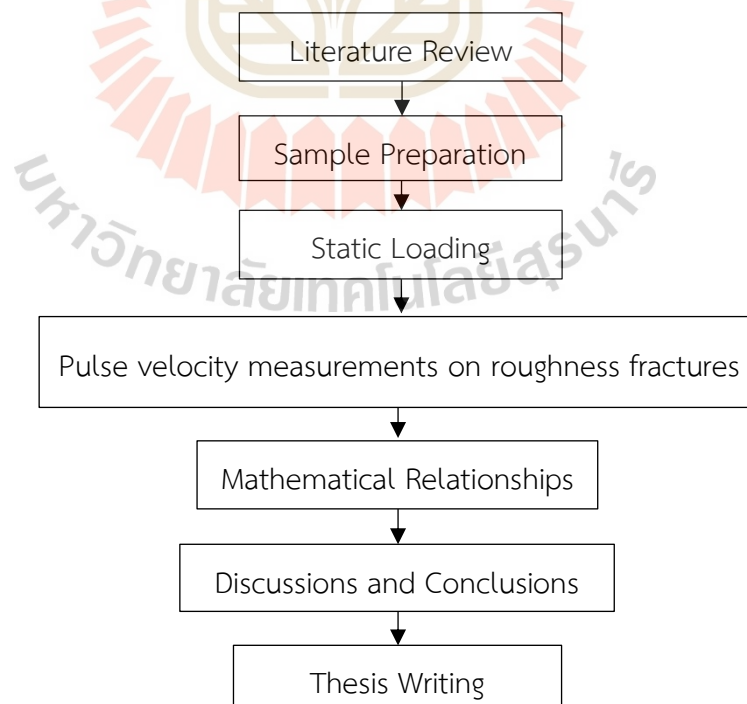
1. Tested specimens are divided into 3 groups (Table 1.1).
2. All specimens can be any core dimensions with length to diameter ratio (L/D) is equal to 5.
3. Testing is made under dry condition.
4. Tension-induced fractures are used to simulate joints.
5. The testing procedure follows the ASTM (D2845-08 and D7012-14) standards.
6. The research findings are published in a conference paper or journal.

Table 1.1 Groups and type of rock samples that are test

Rock type	Location
Sandstone: Phu Phan Formation	Nakhon Ratchasima, Thailand
Sandstone: Sao Khua Formation	Nakhon Ratchasima, Thailand
Sandstone: Phra Wihan Formation	Nakhon Ratchasima, Thailand
Sandstone: Phu Kradung Formation	Nakhon Ratchasima, Thailand
Sandstone: Phu Tok Formation	Nongkhai, Thailand
Marble: Khao Khad Formation	Lopburi, Thailand
Limestone: Khao Khad Formation	Saraburi, Thailand
Travertine: Khao Khad Formation	Saraburi, Thailand
Granite: Tak Batholith	Tak, Thailand

1.4 Research methodology

The research methodology is shown in Figure 1.1, including 7 steps. They include literature review, sample preparation, laboratory testing methods, Pulse velocity measurements on smooth and roughness fractures, analysis and mathematical derivation, discussions and conclusions, and thesis writing.

**Figure 1.1** Research methodology.

1.4.1 Literature review

Literature review is performed to research about ultrasonic measurement and mechanical properties and wave velocity of rocks and effect of fracture roughness, and number of fractures on wave velocity. The sources of information are from journals, technical reports, and conference papers.

1.4.2 Sample preparation

Rock samples test are obtained for 9 specimens. Sample preparations are performed in the laboratory at Suranaree University of Technology. The specimens are prepared to obtain with any core dimension with length to diameter ratio (L/D) equal to 5. The samples are prepared for the physical (wave velocity) tests and the mechanical (static loading) tests. After the preparation of rock samples, total specimens are measured length to find specific gravity (SG) values in each rock specimens. This method is carried on after the specimen was created to obtain artificial fracture every time for accurate measurement of specific gravity.

1.4.3 Static loading

The mechanical testing standard is ASTM D7012-14 (the uniaxial compression test). Unloading method is tested on the rock samples to determine elastic modulus values (Elastic Static) 1 time before creating an artificial fracture and are tested every time after creating an artificial fracture.

1.4.4 Pulse velocity test on roughness fracture

The physical testing standards are density and wave velocity (ASTM D2845). Pulse velocity methods is tested on the rock samples to determine elastic modulus values (Elastic Dynamic) and Poisson's ratio for comparison and prediction between both elastic moduli from static and dynamic methods. The testing method is carried out after cyclic loading testing.

1.4.5 Mathematical Relationships

The results from the laboratory are used to establish the relationship between wave velocity with the parameter of static loading, fracture roughness, and mechanical properties are determined.

1.4.6 Discussions and Conclusions

Discussions are described on the reliability and adequacy of the test data and the correctness of the interpretation and analysis. Comparison of the results and explanations of these problems are described and offered here. To the future research needs are identified. Conclusions from the research are drawn.

1.4.7 Thesis Writing

All research activities and results are documented and compiled in the thesis. This research can be applied to compare the ultrasonic velocity on rocks, the number of fractures, and Young' modulus from laboratory testing.

1.4.8 Discussions, conclusions and thesis writing

Discussions are made on the reliability and adequacies of the approaches used here. Future research needs are identified. All research activities, methods, and results are documented and compiled in the thesis. The research or findings are published in the conference proceedings and journal.

1.5 Thesis content

This research thesis is divided into seven chapters. In the first Chapter I introduce the thesis with describing the background of problems and significance of the study. The research objectives, methodology, scope, and limitations are identified. The second Chapter II describes the results of the literature review about ultrasonic pulse velocity test, the effect of fracture on wave velocity, the effect of physical properties on wave velocity, the effect of mechanical properties on wave velocity and deformations modulus, and joint normal stiffness on rock mass. The third Chapter III describes the sample preparations. The fourth Chapter IV describes the laboratory methodology of static loading and ultrasonic pulse velocity measurement. The fifth Chapter V describes test results of laboratory testing of the static loading tests and ultrasonic pulse velocity measurements. The sixth Chapter VI describes the development of the mathematical relationship between dynamic deformation modulus (E_d) and static deformation modulus (E_s) obtained from the test results in chapter V. The sixth Chapter VII provides the discussions, conclusions, and recommendation on future research studies.

CHAPTER II

LITERATURE REVIEW

2.1 Introduction

This chapter summarizes results of literature review to obtain ultrasonic pulse velocity test, effect of fracture on wave velocity, effect of physical properties on wave velocity, effect of mechanical properties on wave velocity and deformations modulus and joint normal stiffness on rock mass.

2.2 Ultrasonic pulse velocity test

Ultrasonic pulse velocity test is a non-destructive technique since these geophysical methods are easy to use and apply, and gradually more to be used in geotechnical engineering. The technique has been used for many years in several fields, such as geotechniques, underground engineering and mining (Kahraman et al., 2008). Ultrasonic pulse velocity measurements are usually to use in field and laboratory to verify and investigate the dynamic properties of rocks. Most researchers (Kahraman, 2002; Yasar and Erdogan, 2004; Fathollahye et al., 2017) study the correlation between properties of rocks and wave velocity. The wave velocity in rock masses is measured to describe texture and rock structure. The important factors are rock type, mineralogical composition, rock texture, grain size, grain shape, density, porosity, confining pressure, anisotropy, porewater, temperature, weathering, bedding planes, alteration zones, and joint properties (roughness, filling material and water, etc.) (Altindag, 2012).

First using the waves velocities were defined with the pulse transmission method in 1949. Wave velocity measurement testing method can verify the velocity of propagation of elastic waves under laboratory conditions. Yasar and Erdogan (2004) describes that there are three ways which the high and low frequencies of ultrasonic pulse techniques. The P_{wave} and S_{wave} velocities are computed from the distance between transmitter, receiver, and measured travel time. The Pundit testing machine was used to measure a wave velocity index value. The Pundit has a generator, pulse transducer and an electronic counter for time internal measurements (Figure 2.1)

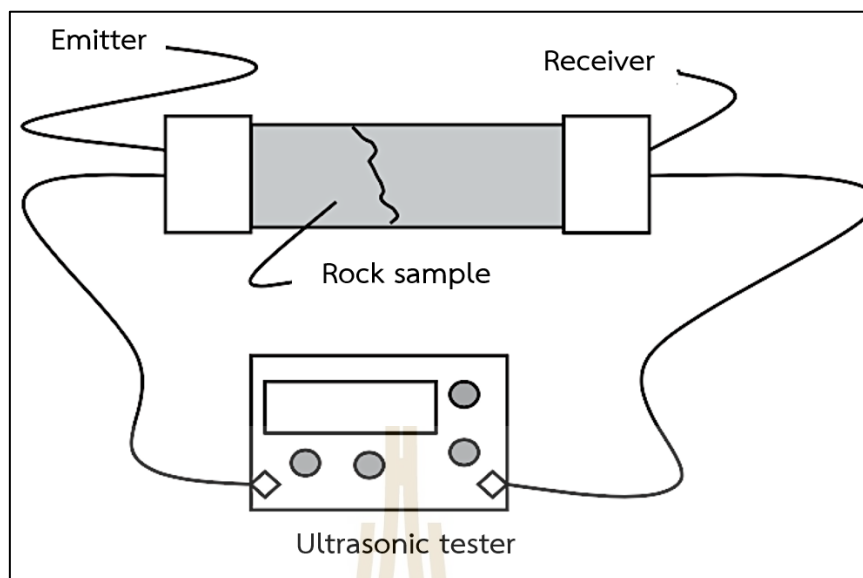


Figure 2.1 Graphic model of wave velocity measuring equipment (the PUN- DIT) (Yasar and Erdogan, 2004).

2.3 Effect of fracture on wave velocity

Field of rock engineering is important to find out fracture zones and approximation on any location, size, and physical properties. For discontinuities in rock mass, for example, fractured zones and faults, which affect the strength of rock masses. Usually, materials filling fractures will have low velocity and low density compared with the surrounding intact rocks. For this reason, P-waves will be transmitted through the fractured zones affected by the amplitude, velocity, and waveform (Watanabe and Sassa, 1995). The effects depend on fractures, the thickness, the distribution, and physical properties of rocks. Therefore, P-wave is helpful for exploration methods. It is non-destructive and can determine fractures in rock masses.

Kahraman (2002) studies the effects of fracture roughness on P-wave velocity. Wave velocity test is performed with three different rocks. There are four different roughness. A fracture roughness coefficient (FRC) was set for each type (Table 2.1). The fracture roughness coefficient values alter between 0 and 4. The results of the tests are presented in Table 2.2.

Table 2.1 Fracture surface pattern model (Kahraman, 2002).


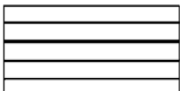
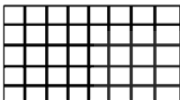
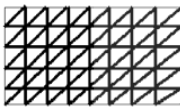
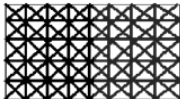
The pattern of fracture surface	Fracture roughness coefficient (FRC)	Description
	0	Smooth
	1	Low roughness
	2	Medium roughness
	3	High roughness
	4	Very High roughness

Table 2.2 P-wave velocity tests result (Kahraman, 2002).

FRC	P-wave velocity (km/sec)		
	Granite	Marble	Travertine
0	4.67	5.96	4.78
1	4.65	5.93	4.73
2	4.61	5.91	4.71
3	4.54	5.85	4.61
4	4.18	5.62	4.23

The results of the wave velocity are analyzed by least squares regression. The equation is suitable, the 95% confidence limits, and the correlation coefficients (R^2) were defined for each equation. The P-wave velocities were related to fracture roughness coefficient values for each rock type. The graphs of the P-wave velocities as a function of the fracture roughness coefficient values are shown in Figures 2.2 to 2.4. The figures show polynomial relationships between the fracture roughness coefficient values and the P-wave velocities. Many researchers (Watanabe and Sassa, 1995; Boadu, 2000; Kahraman, 2001) who studied the effect of fracture on wave velocity show the same trend. In the earliest stage, the P-wave velocities gradually reduced. The P-wave increases in the fracture roughness coefficient values. The correlation coefficients and

the regression equations are presented in Table 2.3 The correlation was introduced relationships between two variables and coefficients are high for all rock types.

Table 2.3 Regression equations for each rock types (Kahraman, 2002).

FRC	Regression equation	Coefficient of correlation (R^2)
Granite	$V_p = -0.022(\text{FCR})^2 + 0.02\text{FRC} + 4.66$	0.990
Marble	$V_p = -0.017(\text{FCR})^2 + 0.013\text{FRC} + 5.95$	0.982
Travertine	$V_p = -0.03(\text{FCR})^2 + 0.03\text{FRC} + 4.76$	0.976

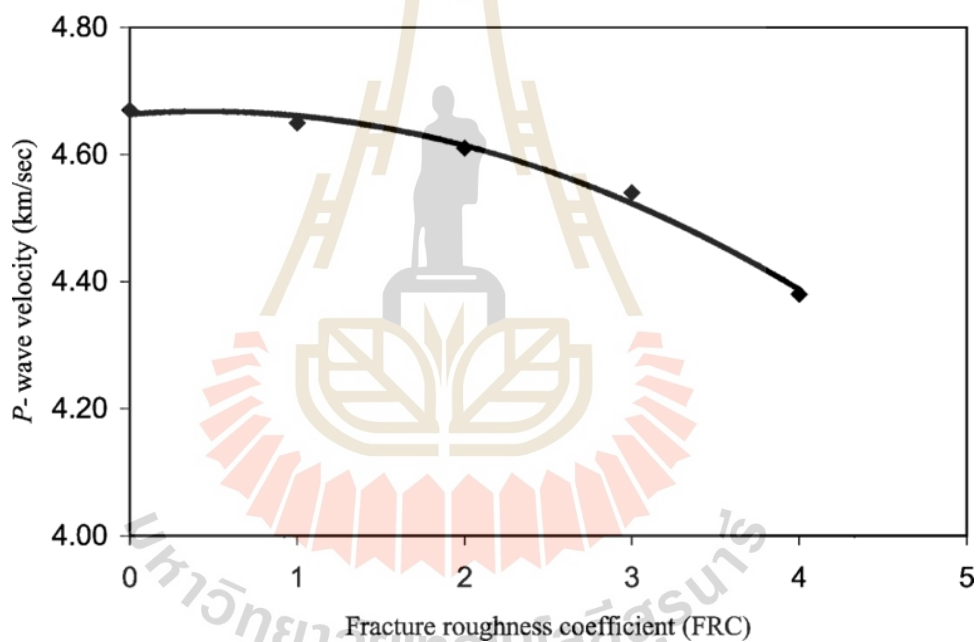


Figure 2.2 Results of granite between P-wave velocity and FRC. (Kahraman, 2002).

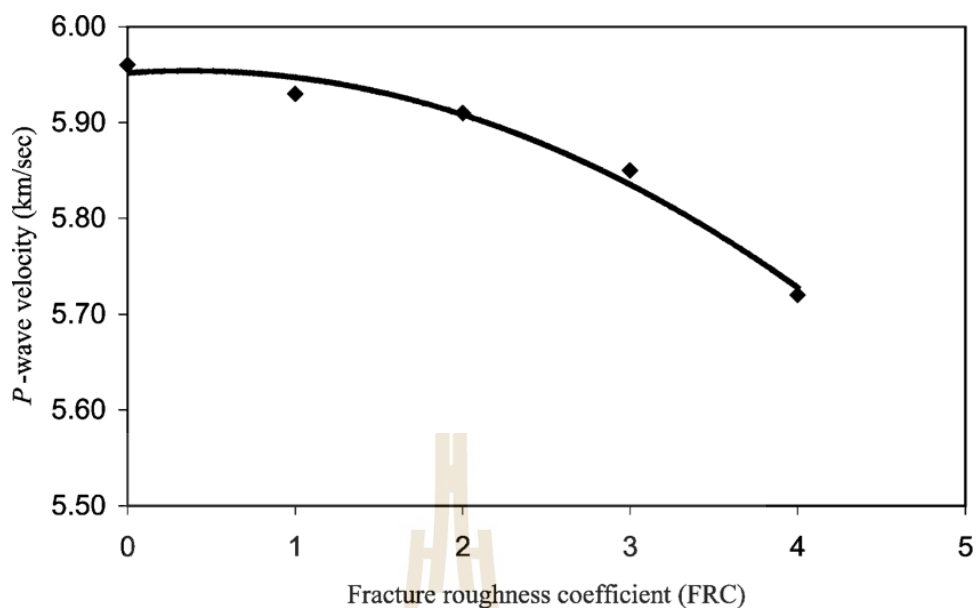


Figure 2.3 Results of marble between P-wave velocity and FRC (Kahraman, 2002).

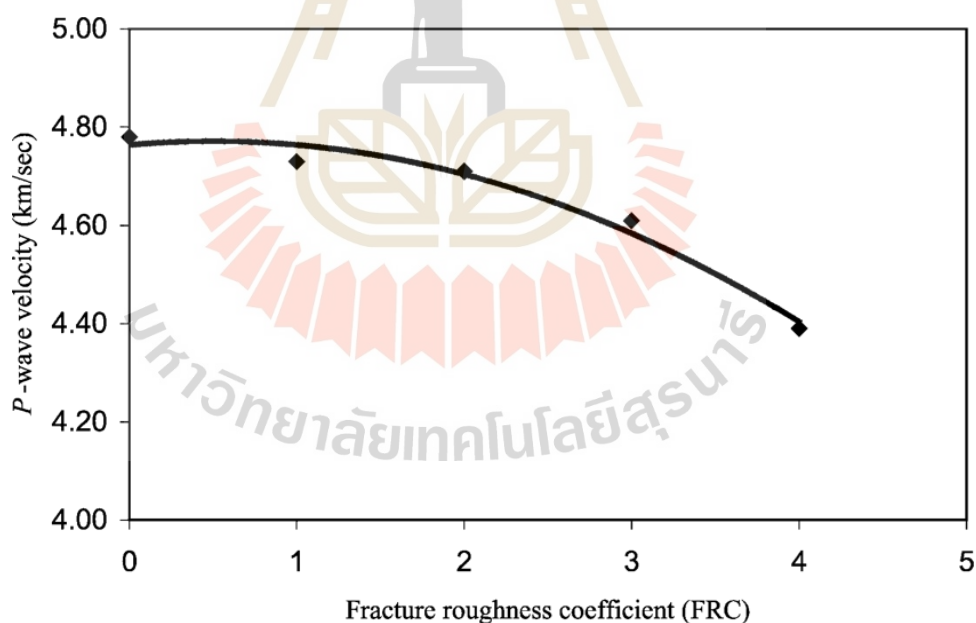


Figure 2.4 Results of travertine between P-wave velocity and FRC (Kahraman,2002).

P-wave velocity measurements were used to assess the rock mass quality. Fathollahye et al. (2017) described various factors, such as joint spacing, which may affect P-wave velocity. This work shows P-wave velocity changing with joint spacing in

Andesite samples. The physical properties of the samples were defined artificial fractures of 2 and 5 centimeters spacing by created in the samples. To carry out the measurements, transducers were set on the top and bottom of the samples. The results show a good relationship between the wave velocity, number of fractures and their spacing, showing that the reduction of wave velocity depends on the joint spacing more than the number of fractures.

P-wave velocities have been used to measure in the direction parallel to longitudinal axis of the core samples and then artificial joints were created by cutting each sample normal to the axis. The fractures were increased by addition like a disk shape samples with lengths of 2 and 5 centimeters between the two portions (Figures 2.5 and 2.6). The step was replicated for 9 sets of Andesite with 0.1 MPa axial loading. Measurements were carried out according to the ASTM standard (D 2845-00). Wave velocities were tested on the sets of samples as shown in Table 2.4. The results show the reductions in the P-wave velocity by inverse with the fracture number. Figure 2.7 shows P-wave velocity comparing with the increasing fractures with different spacing.

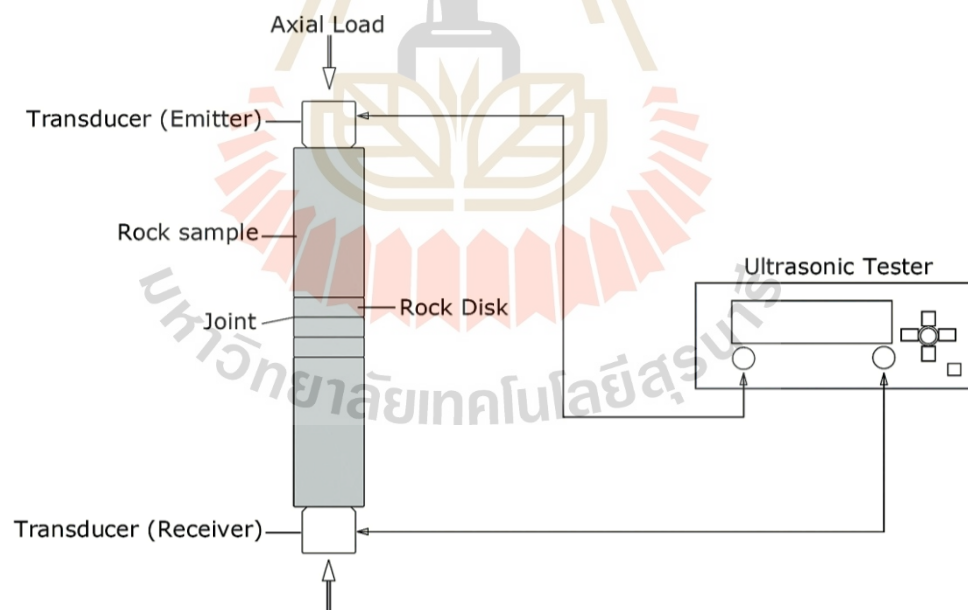


Figure 2.5 V_p measurement on samples in laboratory (Fathollahye et al., 2017).

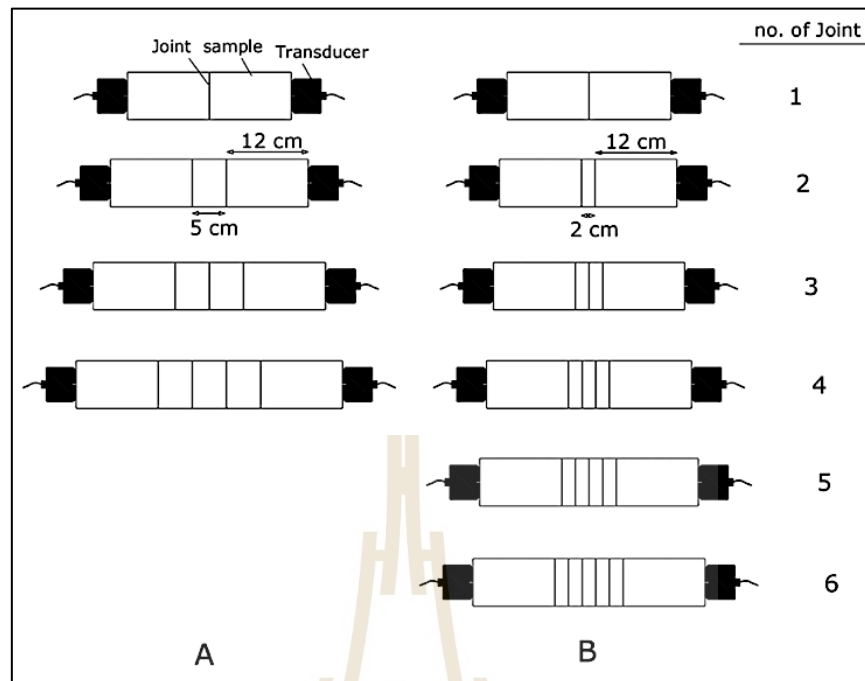


Figure 2.6 Increasing fractures with different spacing (Fathollahye et al., 2017).

Table 2.4 Results of V_p measurement on samples (Fathollahye et al., 2017).

No. of joint		Samples									
		G1	G2	G3	G4	G5	G6	G8	G9	G16	
0	V_p (m/s)	Spacing = 2 cm	5778	5764	5689	5685	5669	5869	5766	5536	6024
1			5522	5459	5284	5409	5479	5601	5563	5417	5883
2			5478	5366	5291	5373	5453	5574	5437	5359	5830
3			5430	5321	5246	5340	5408	5520	5404	5346	5764
4			5356	5205	5025	5269	5360	5453	5366	5315	5725
5			5318	5131	4776	5215	5283	5404	5246	5280	5684
6		5256	4976	4358	5136	5139	5260	5105	5177	5430	
1		Spacing = 5	5522	5459	5284	5409	5479	5601	5563	5417	5883
2			5442	5328	5253	5362	5407	5556	5550	5342	5765
3			5423	5289	5226	5330	5389	5520	5542	5331	5716
4	5394		5275	5199	5287	5356	5473	5522	5308	5685	

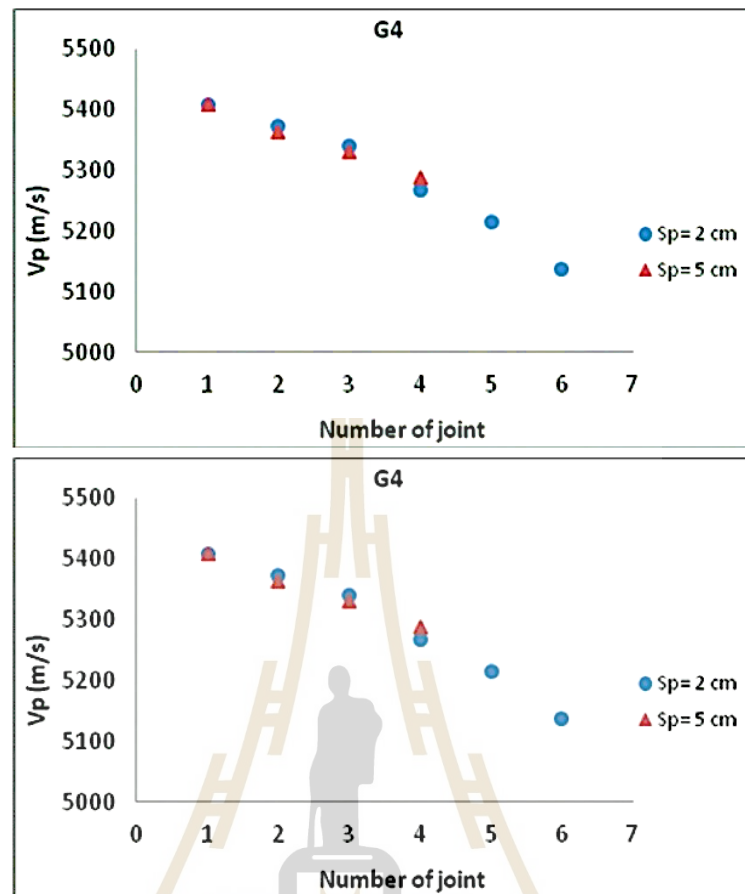


Figure 2.7 P-wave velocity with different fracture spacings (Fathollahye et al., 2017).

To estimate the variation of P-wave velocity with the increasing the number of fractures by different spacing of rocks, the velocity reduction ratio (VRR%) was imposed as follows:

$$VRR\% = \frac{V_0 - V_1}{V_0} \times 100 \quad (2.1)$$

The results show that the rate is different for every different joint spacings. However, VRR% had an increasing trend with increasing number of fractures. Table 2.5 presents the VRR% in each processed. Figures 2.8 gives the average of VRR% comparing with joint number. The results show that the rate of velocity reduction ratio (VRR%) for shorter spacing is more than the large spacing.

Based on the three fractures, wave velocity reduced in the spacing of 5 centimeters is more than that of 2 centimeters due to the effect of spacing length on wave velocity reduction.

Table 2.5 P-wave VRR% in different joint numbers (Fathollahye et al., 2017).

No. of joint			Samples								VRR% (average)	
			G1	G2	G3	G4	G5	G6	G8	G9		G10
1	VRR%	Spacing = 2 cm	4.43	5.29	7.12	4.86	3.35	4.57	3.51	2.15	2.35	4.41
2			5.19	6.91	7.00	5.49	3.81	5.03	5.70	3.20	3.23	5.29
3			6.02	7.69	7.79	6.07	4.61	5.95	6.27	3.43	4.32	5.98
4			7.31	9.70	11.67	7.32	5.45	7.09	6.93	3.99	4.97	7.43
5			7.96	10.98	16.05	8.27	6.81	7.93	9.01	4.63	5.65	8.96
6			9.04	13.67	23.40	9.66	9.35	10.38	11.46	6.49	9.87	11.68
1		Spacing = 5 cm	4.43	5.29	7.12	4.86	3.35	4.57	3.51	2.15	2.35	4.41
2			5.82	7.57	7.67	5.68	4.62	5.34	3.74	3.51	4.31	5.49
3			6.15	8.24	8.14	6.25	4.94	5.95	3.88	3.71	5.12	5.91
4			6.65	8.49	8.62	7.00	5.52	6.75	4.22	4.12	5.63	6.42

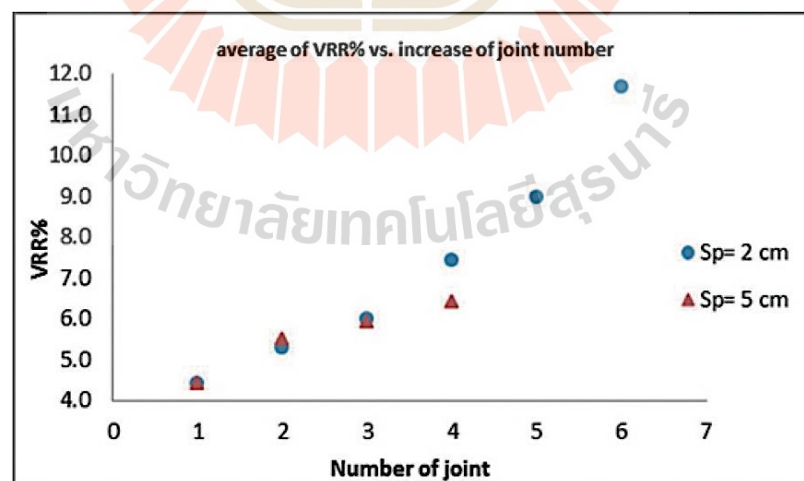


Figure 2.8 Average of VRR% compare increasing of fracture number with different spacing in Andesite rock samples (Fathollahye et al., 2017).

2.4 Effect of physical properties on wave velocity

Physical properties for example porosity, density and permeability have a pointed influence on the properties of rocks. Therefore, there have been used geophysical techniques to determine such properties by seismic or sonic measurements for rocks characterization. The velocity measurement has been performed to define the geotechnical properties of rocks, which is a simple and easy way to use and apply in the field and laboratory (Khandelwal, 2013). The ultrasonic velocity test depends on measuring the propagation time of a P-wave in the longitudinal direction according to Rahmouni, et al. (2013). Some researchers (Han et al.,1986; Klimentos, 1991; Tuğrul and Zarif,1999; Starzec,1999; Gao et al.,2000; Vanorio et al.,2003; Sousa et al.,2005; Rao et al., 2006; Kurtulus et al.,2012; Gupta and Sharma, 2012) determine the effect of physical properties on wave velocity and predict the correlation between P-wave velocity and the porosity, permeability, density, and grain size of rocks.

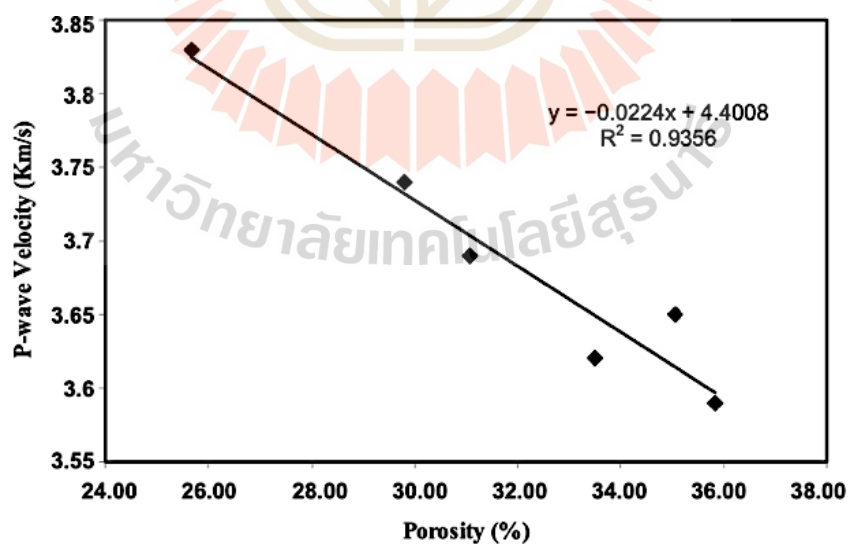
The study of P and S wave propagation in a dry and saturated material has been carried out to assess the physical properties of materials. Observation of the ultrasonic pulse velocity (UPV) with dry and saturated rocks by Kahraman (2007), who related the UPVdry and UPVsat for all rocks, with different porosity values. Rocks are often absorbed in the P-wave and S-wave. In a P-wave, the wave starts in the direction of propagation and affects the rock volume. In S-wave, the vibration propagates in a plane normal to the direction of propagation, it is slower than the P-wave and cannot transmit in liquid. The transmitting time of the waves depends on the rock density. The correlation between wave velocity and density in rocks is considered as a linear. It depends on the porosity and the possibly anisotropic of the material particles. Density and porosity are major parameters for the quality of structuring in rocks.

The velocity of ultrasonic moving in rock material depends on the elastic properties and density. The quality of some materials is correlated with elastic for measurement of ultrasonic pulse velocity in rocks which can be used to specify quality and define the elastic properties (Yagiz, 2011). The wave velocity is computed from the time taken on the wave to transmit the measuring distance between the transmitter and the receiver. In apply, only the porosity of a rock can be measured. The space between the grains and microcracks is controlled by the volume of porosity. The porosity controls all physical parameters, such as permeability, density, thermal conductivity, etc. Table 2.6 shows these samples having differences in porosity.

Table 2.6 Physical properties of calcarenite rocks (Rahmouni et al., 2013).

Sample	P-wave velocity		Density		Porosity ϕ (%)
	V_P (km/s)		ρ (g/cm ³)		
	Dry	Saturated	Dry	Saturated	
1	3.8	3.83	1.75	2	25.69
2	3.7	3.74	1.68	1.97	29.82
3	3.62	3.69	1.64	1.95	31.07
4	3.64	3.62	1.59	1.92	33.50
5	3.61	3.65	1.6	1.95	35.07
6	3.56	3.59	1.6	1.94	35.83

The average porosity of the samples is 31.83%. The P-wave velocity depends on porosity, mineral composition, microcracks, and moisture content. The velocity measured in a macroscopic sample varies by solid-solid, fluid-fluid, or solid-fluid interfaces, which is an average of the velocity in the fluid. The low value of the P-wave velocity is earned for dry samples and the high value is earned for the samples saturated.

**Figure 2.9** P-wave velocity compared porosity of dry samples (Rahmouni, et al., 2013).

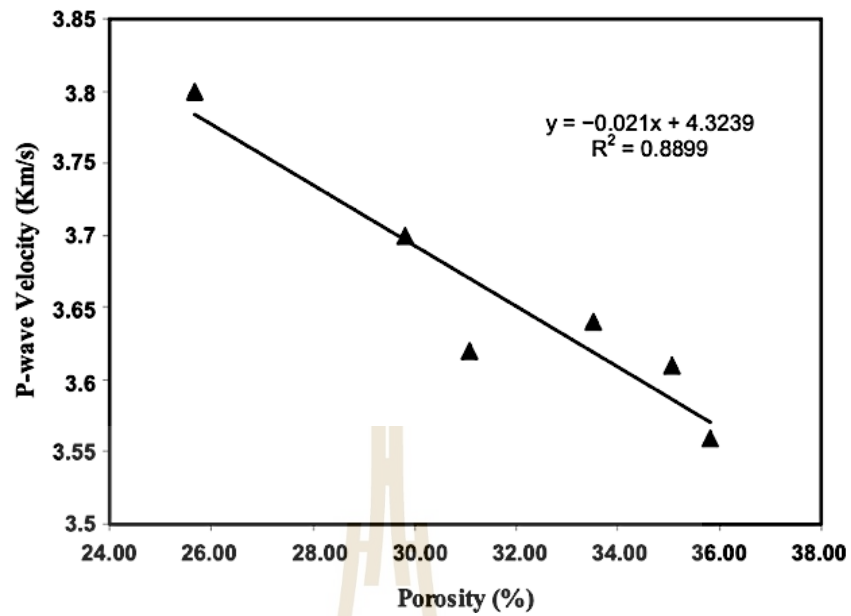


Figure 2.10 P-wave velocity compared with porosity of saturated samples (Rahmouni, et al., 2013).

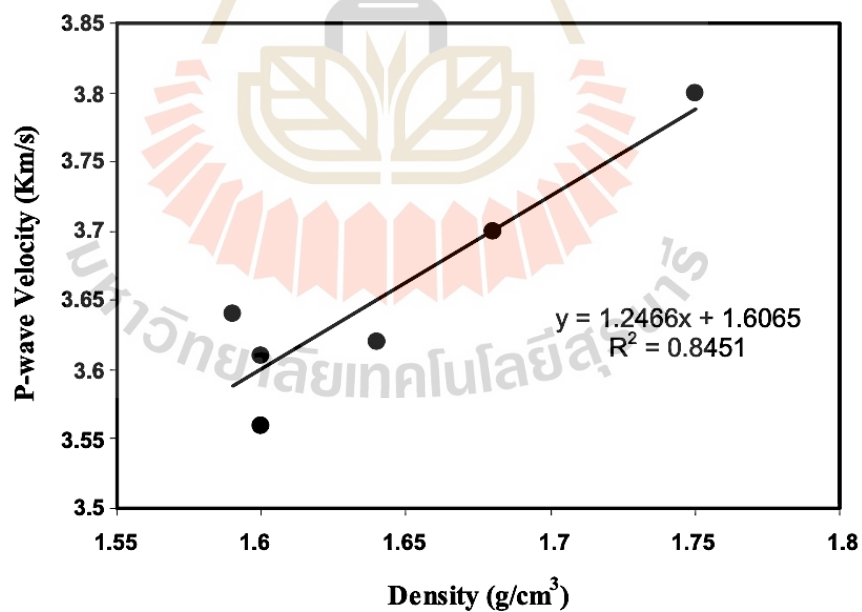


Figure 2.11 P-wave velocity compared with density of dry samples (Rahmouni, et al., 2013).

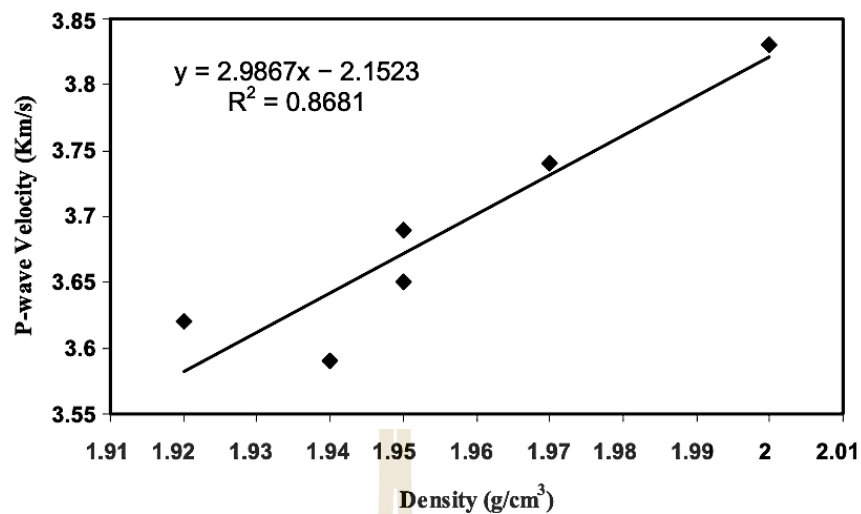


Figure 2.12 P-wave velocity compared with density of dry samples (Rahmouni, et al., 2013).

Many researchers who study the P-wave velocities with dry and saturated states that V_p (dry) < V_p (saturated), also observed that the wave velocity is higher in the saturated state for the limestone. A regression analysis was determined to describe the correlations between P-wave with density and porosity. The P-wave velocity of the dry and saturated calcarenite decreased as the porosity is increasing, as shown in Figures 2.9 and 2.10. The velocity and density will increase concurrently for both dry and saturated samples, as shown by a linear relationship in Figures 2.11 and 2.12.

2.5 Effect of mechanical properties on wave velocity

Yasar and Erdogan (2004) described the wave velocity of rocks which was related to the uniaxial compressive strength (UCS), density (ρ), and Young' modulus (E) for each rock type. In every case, the good suitable relations were obtained to be linearity. Good correlations were found between wave velocity index and other properties of rocks. The results are presented in Table 2.7. The results between wave velocity index and UCS, Young's modulus, and density are depicted in Figures 2.13 to 2.15. The result is corresponding with the testing result of Moradian (2009), Yilmaz et al. (2011), Selçuk and Nar (2016), and Daoud et al. (2017) who predict the uniaxial compressive strength of intact rocks by using ultrasonic pulse velocity. Showing the same results of the regression equation, such as the relation between wave velocity with UCS and elastic Young' modulus.

Table 2.7 Regression analysis results (Yasar and Erdogan, 2004).

Parameters to be related	Regression equation ($Y = AX \pm B$)	R^2
Wave Velocity — UCS	$WV = 0.0317 \sigma_c + 2.0195$	0.80
Wave Velocity — E	$WV = 0.0937E + 1.7528$	0.86
Wave Velocity — ρ	$WV = 4.3183 \rho - 7.5071$	0.81

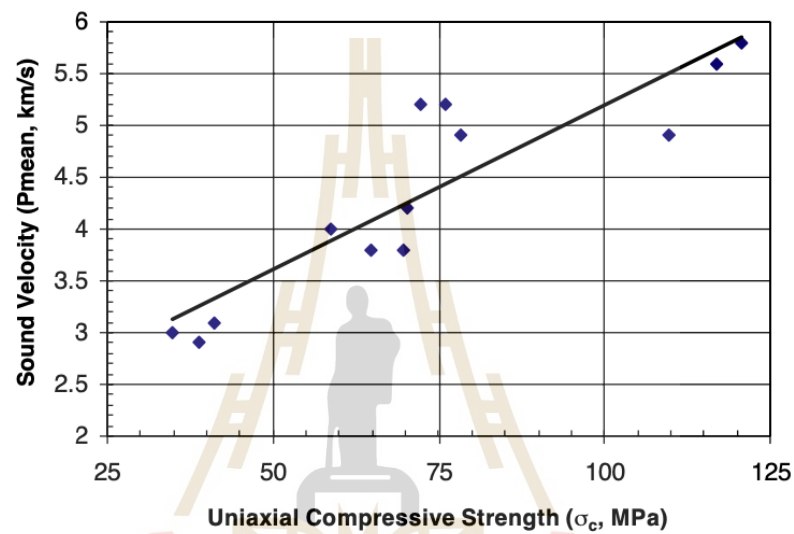


Figure 2.13 Correlation of wave velocity and UCS (Yasar and Erdogan, 2004).

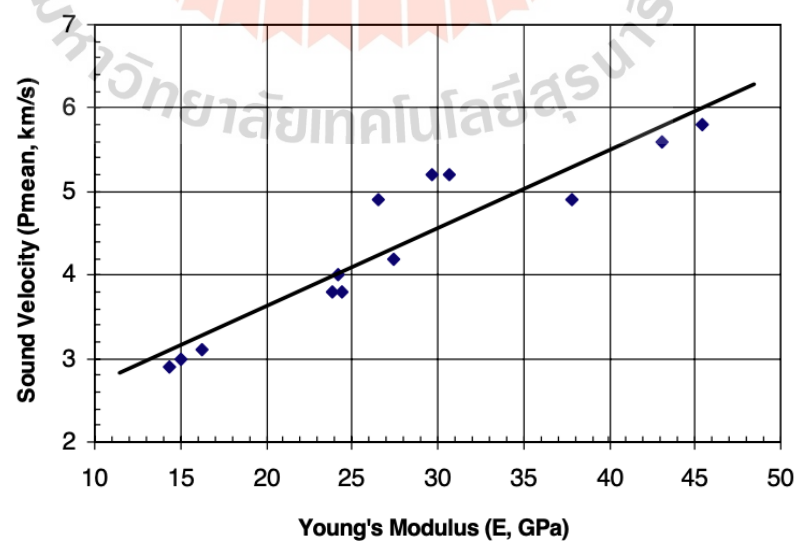


Figure 2.14 Correlation of wave velocity and Young's modulus (Yasar and Erdogan, 2004).

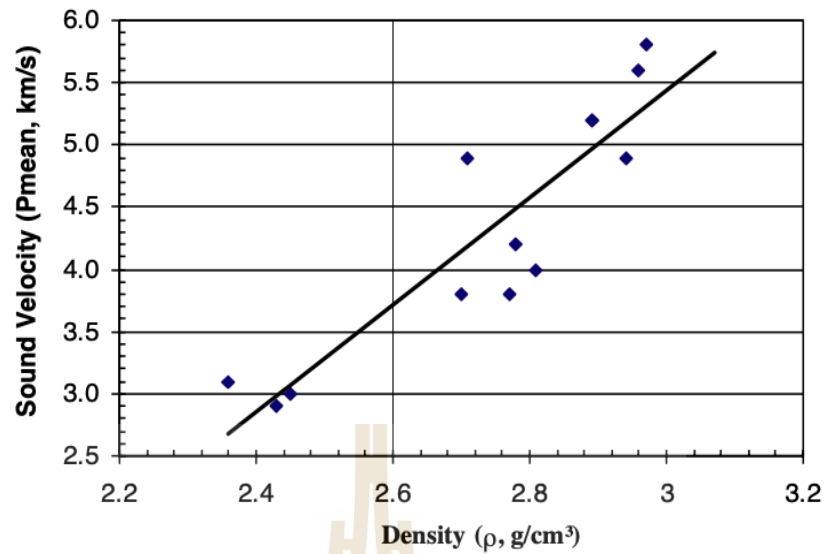


Figure 2.15 Correlation of wave velocity and density (Yasar and Erdogan, 2004).

The test results agree with those of Altindag (2012). Many equations are appraised to assess the uniaxial compressive strength of rock from the P-wave velocity, mostly equations of linear and relationships between the compressive strength and P-wave velocity. A correlation was found between the compressive strength and P-wave velocity as shown in Figure 2.16. The equation of the curve is $UCS = 12.743V_p^{1.194}$. The correlation coefficient of the relationship is 0.76. The analysis used in this study relying on the relationship between the P wave and other properties of intact rocks were based on the data obtained from different studies.

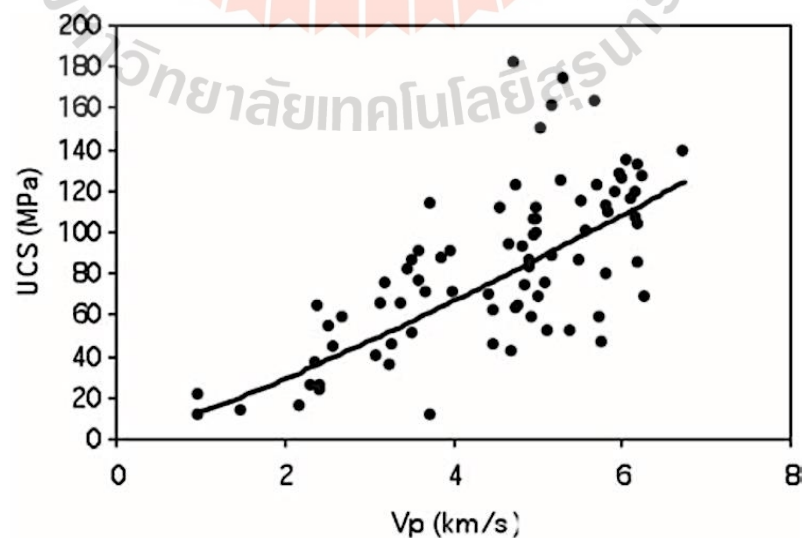


Figure 2.16 Relative result between P-wave velocity and UCS of rocks (Altindag, 2012).

2.6 Deformations modulus and joint normal stiffness on rock mass

Goodman (1970) has proposed an equation to evaluate the elastic constants for an equivalent continuous material representative of a rock mass. However, the equation only can evaluate in one set of joints. The equation is:

$$\frac{1}{E_r} = \frac{1}{k_n s} + \frac{1}{E_n} \quad (2.2)$$

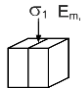
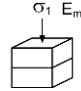


where E_r is the rock deformation modulus, k_n is the joint normal stiffness, s is the average joint spacing and E_n is the equivalent deformation modulus.

Thaweeboon et al. (2017) has modified and improved the equation of Goodman (1970) to determine deformation modulus in different directions.

$$\frac{1}{E_m} = \frac{1}{k_n s} + \frac{1}{E_i} \quad (2.3)$$

where E_m is the jointed rock deformation modulus, E_i is the intact deformation modulus, s is the joint spacing, k_n is the joint normal stiffness and N is a parameter which value depends on direction of joint set as show in Table 2.8.

Table 2.8 Parameter N defined for modified equation by Thaweeboon et al. (2017).

Number of joint sets	Orientation of joint set to σ_1	Case	N
1	1 parallel		0.5*
1	1 normal		1.0* (original Goodman)
2	1 parallel, 1 normal		1.5
2	2 parallels, 1 normal		2.0*

*Verified by the test results

The results show that the equation of Goodman (1970) gives a good prediction to determine deformation modulus for single joint set specimens with normal joint to the principal axis but cannot determine the deformation modulus of specimens with more than one joint set. Goodman (1970) equation is developed to define the deformation modulus with three principal directions. The parameter N is presented which value depends on joint set direction. The presented equation can only estimate the deformation modulus in the normal and parallel directions to the joint planes.

Results of Seephan (2018) agree with those of the Thaweewoon's modified equation which can appropriately describe the deformation modulus normal to the joints planes for more than one joint set specimens. The deformation modulus with roughness fractures and smooth fractures gives a good relationship on the test data of with R^2 more than 0.9. The roughness fractures show higher deformation modulus values than the smooth fractures.

Starzec (1999) studies the dynamic elastic properties of crystalline rocks. The results are obtained from the investigation of ultrasonic velocity measurement on igneous and metamorphic rocks from Sweden 300 samples. The linear correlation between the static and dynamic elastic modulus by using ultrasonic velocity measurement for determination the elastic modulus for the examination of rock specimens. The correlation between the dynamic and static modulus. As predicted, the dynamic modulus was constantly higher than the static modulus as show in Figure 2.17 according to Mockovčiaková and Pandula, (2003), Onalo et al., (2018), and Moradian, (2009).

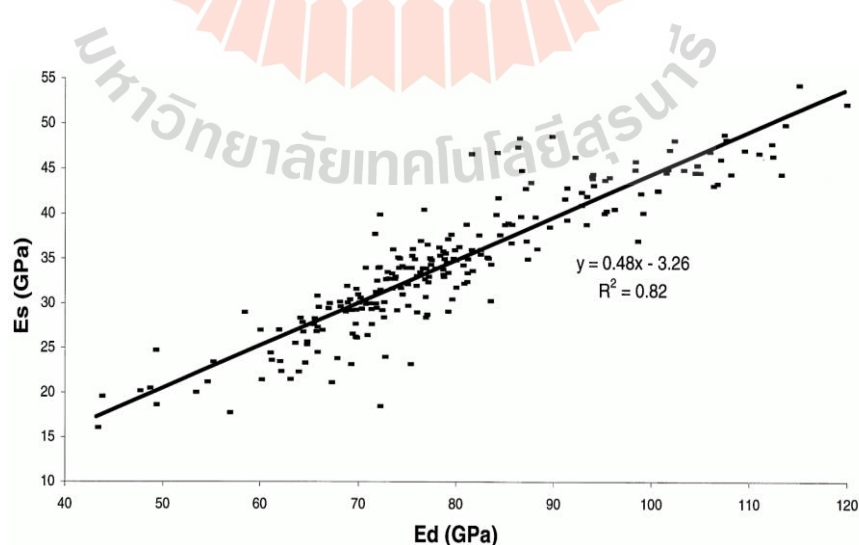


Figure 2.17 Relationship between static E_s and dynamic E_d moduli for 5 different crystalline rock types (Starzec, 1999)

Kulatilake et al. (2001) has presented the results of the experiments and numerical simulations using Particle Flow Code (PFC 3D), which were carried on studying the behavior of jointed blocks of model material under uniaxial loading. The experiment has shown that having joints reduces the strength of rock mass when compared to intact rock. The strength reduction is controlled by joint geometry configuration and intact and joint mechanical properties. The jointed blocks of the model material with the fracture were examined by the variation of the uniaxial compressive strength (UCS). Hoek and Brown (1980,1997) presented an empirical criterion to estimate rock mass strength. Even though they investigated anisotropy of rock mass strength, the rock mass failure criterion used in practice suppose isotropy.

PFC 3D gives the equations that can be used to make estimates of the particle stiffness and bond strength from values of the macro mechanical parameters defined in laboratory testing:

$$E = \frac{K_n}{4R} \quad (2.4)$$

where E is the Young's modulus as obtained from laboratory tests, K_n is the normal stiffness of the particles and R is the particle radius.

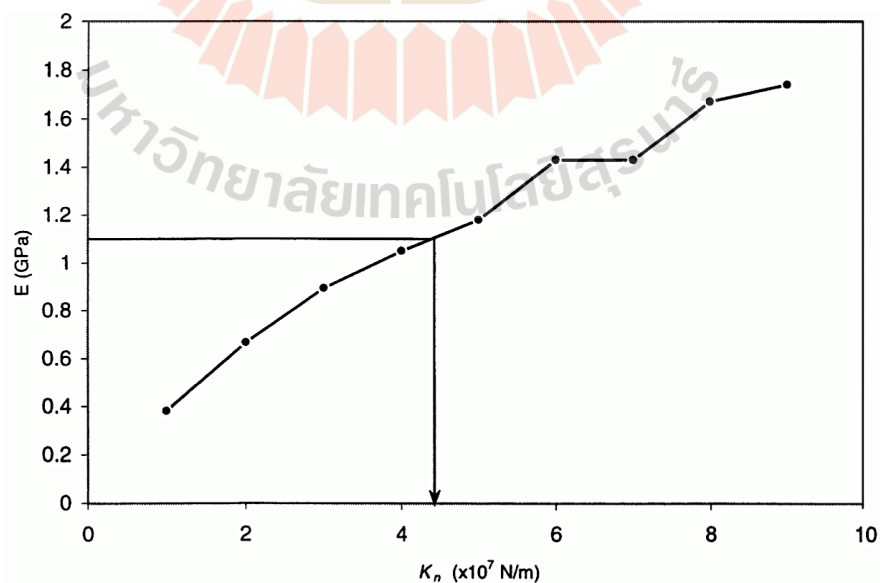


Figure 2.18 Calibration plotting show variation of Young's Modulus with joint normal stiffness of the particles (Kulatilake et al., 2001)

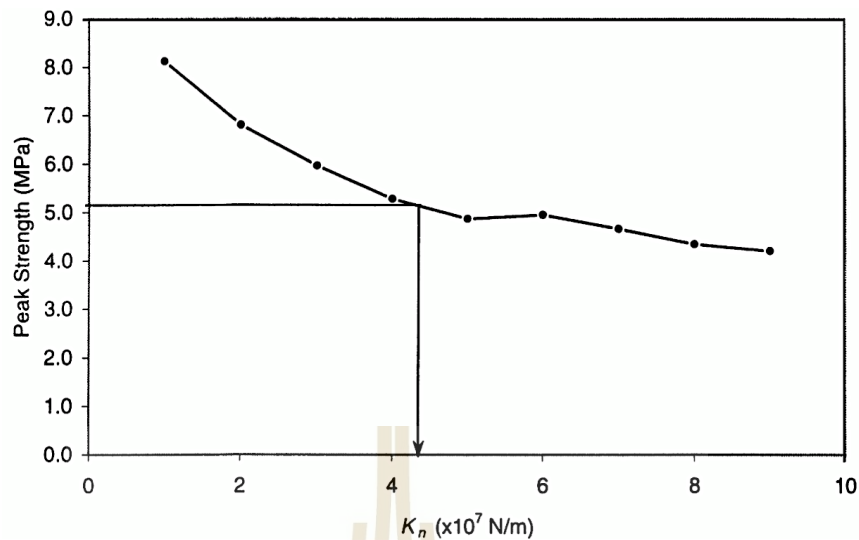


Figure 2.19 Calibration plotting show the variation of Peak Uniaxial Strength with joint normal stiffness of the particles (Kulatilake et al., 2001)

The equation shows that Young's modulus is inversely related to the particle radius and directly related to the particle stiffness. Figures 2.18 and 2.19 show the calibration curves for the normal particle stiffness. By showing the Young's modulus and the peak uniaxial strength of normal particle stiffness. A relation is approximately linear between the Young's modulus and the normal stiffness as was predicted from the equation (4).

Table 2.9 Linear relationship between static (E_{stat}) and dynamic (E_{dyn}) modulus ($E_{stat} = a \cdot E_{dyn} - b$) by Davarpanah et al. (2020).

a	b	Rock type	Refs.
1.137	9.68	Granite	Belikov et al. (1970)
1.263	29.5	Igneous and metamorphic rocks	King (1983)
0.64	0.32	All types	Eissa and Kazi (1988)
0.48	3.26	Crystalline rocks	McCann and Entwisle (1992)
0.74	0.82	All types	Eissa and Kazi (1988)
1.05	3.16	All types	Christaras et al. (1994)
1.153	15.2	All types	Nur and Wang (1999)
0.86	2.085	Crystalline rocks	Brottons et al. (2014)
0.932	3.42	All types	Brottons et al. (2016)

Davarpanah et al. (2020) has studied and compile many previous researching about the relationship between dynamic and static deformation modulus of intact rock. Relationships are developed between dynamic and static Young's moduli: $E_{stat} = a \cdot E_{dyn} - b$, as shown in Table 2.9. The static modulus is dependent of the dynamic modulus, as shown in Figure 2.20.

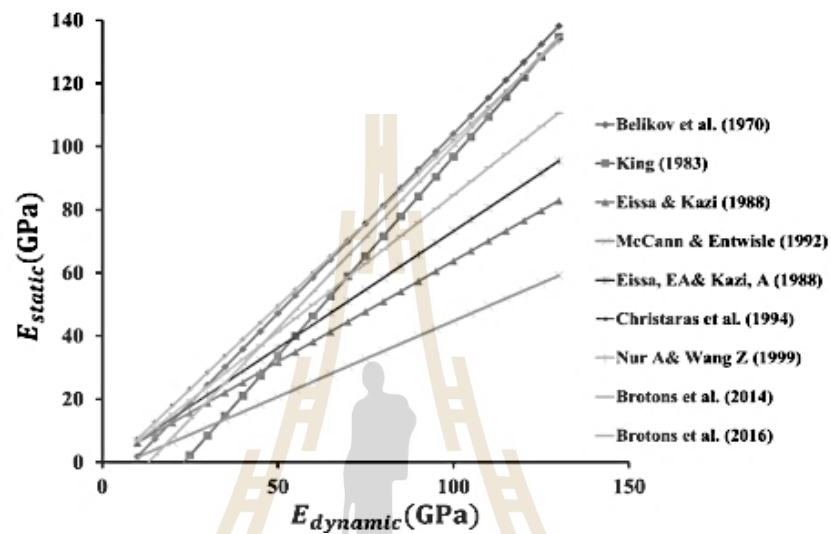


Figure 2.20 Plot of relationship between measured static and dynamic modulus of elasticity: $E_{stat} = a \cdot E_{dyn} - b$ (Davarpanah et al., 2020).

CHAPTER III

SAMPLE PREPARATION

3.1 Introduction

This chapter describes information of rock samples, and sample preparation for mechanical (static loading) tests and dynamic (wave velocity) tests of physical and mineralogy properties are given.

3.2 Rock sample

The rock samples used in this study are prepared from nine rock types dividing into three groups: clastic, carbonate, and plutonic. They are commonly found in Thailand. Table 3.1 gives the rock types, appeared formation, and locations of rock samples where have been collected to examine. Each rock group can classify from the origin, mineral composition in Table 3.2, and texture as show in Figure 3.1.

Table 3.1 Rock samples used for this study.

Rock Type	Code	Rock Unit	Location	Period
White Quartz Sandstone	JK_{pw}	Phra Wihan Formation	Nakhon Ratchasima	Cretaceous
Sandstone	K_{sk}	Sao Khua Formation	Nakhon Ratchasima	
Sandstone	KT_{pt}	Phu Tok Formation	Nongkhai	
Quartz Sandstone	K_{pp}	Phu Phan Formation	Nakhon Ratchasima	Cretaceous-Jurassic
Calcareous Lithic Sandstone	J_{pk}	Phu Kradung Formation	Nakhon Ratchasima	Jurassic
Marble	P_{kd}	Khao Khad Formation	Lopburi	Permian
Limestone			Saraburi	
Travertine				
Granite	C_{gr}	Tak Batholith	Tak	Carboniferous-Cretaceous

Table 3.2 Mineral compositions of rock specimens.

Rock Types	Mineral compositions (weight %)	
Phra Wihan sandstone	Quartz	83.49
	Kaolinite	3.87
	Muscovite	0.52
	Albite	4.12
	Anorthite	1.01
	Microcline	3.14
	Calcite	0.33
	Oligoclase	0.00
	Chlorite	3.43
Sao Khua sandstone	Quartz	37.23
	Kaolinite	3.92
	Muscovite	7.45
	Albite	30.5
	Anorthite	5.65
	Microcline	10.5
	Calcite	0.00
	Oligoclase	2.62
	Chlorite	9.19
Phu Tok sandstone	Quartz	75.60
	Kaolinite	9.09
	Muscovite	9.09
	Albite	2.36
	Anorthite	0.26
	Microcline	1.67
	Calcite	0.00
	Oligoclase	1.05
	Chlorite	0.07

Table 3.2 Mineral compositions of rock specimens (Cont.).

Rock Types	Mineral compositions (weight %)	
Phu Phan sandstone	Quartz	85.55
	Kaolinite	7.01
	Muscovite	0.90
	Albite	3.80
	Anorthite	0.00
	Microcline	0.50
	Calcite	0.00
	Oligoclase	0.00
	Chlorite	2.24
Phu Kradung sandstone	Quartz	36.69
	Kaolinite	2.91
	Muscovite	11.49
	Albite	23.03
	Anorthite	2.80
	Microcline	4.26
	Calcite	0.22
	Oligoclase	10.01
	Chlorite	8.59
Khao Khad marble	Calcite	95.12
	Quartz	0.21
	Dolomite	3.24
	Chalcopyrite	1.43
	Fluorite	0.00
	Microcline	0.00
	Actinolite	0.00

Table 3.2 Mineral compositions of rock specimens (Cont.).

Rock Types	Mineral compositions (weight %)	
Khao Khad limestone	Calcite	89.35
	Quartz	0.00
	Dolomite	7.88
	Chalcopyrite	0.00
	Fluorite	0.15
	Microcline	1.89
	Actinolite	0.73
Khao Khad travertine	Calcite	97.18
	Quartz	0.10
	Dolomite	1.92
	Chalcopyrite	0.08
	Fluorite	0.00
	Microcline	0.00
	Actinolite	0.00
Tak granite (C _{gr})	Quartz	36.22
	Muscovite	5.53
	Chlorite	1.17
	Albite	17.17
	Orthoclase	27.28
	Anorthite	10.28
	Diopside	1.18
	Microcline	0.00

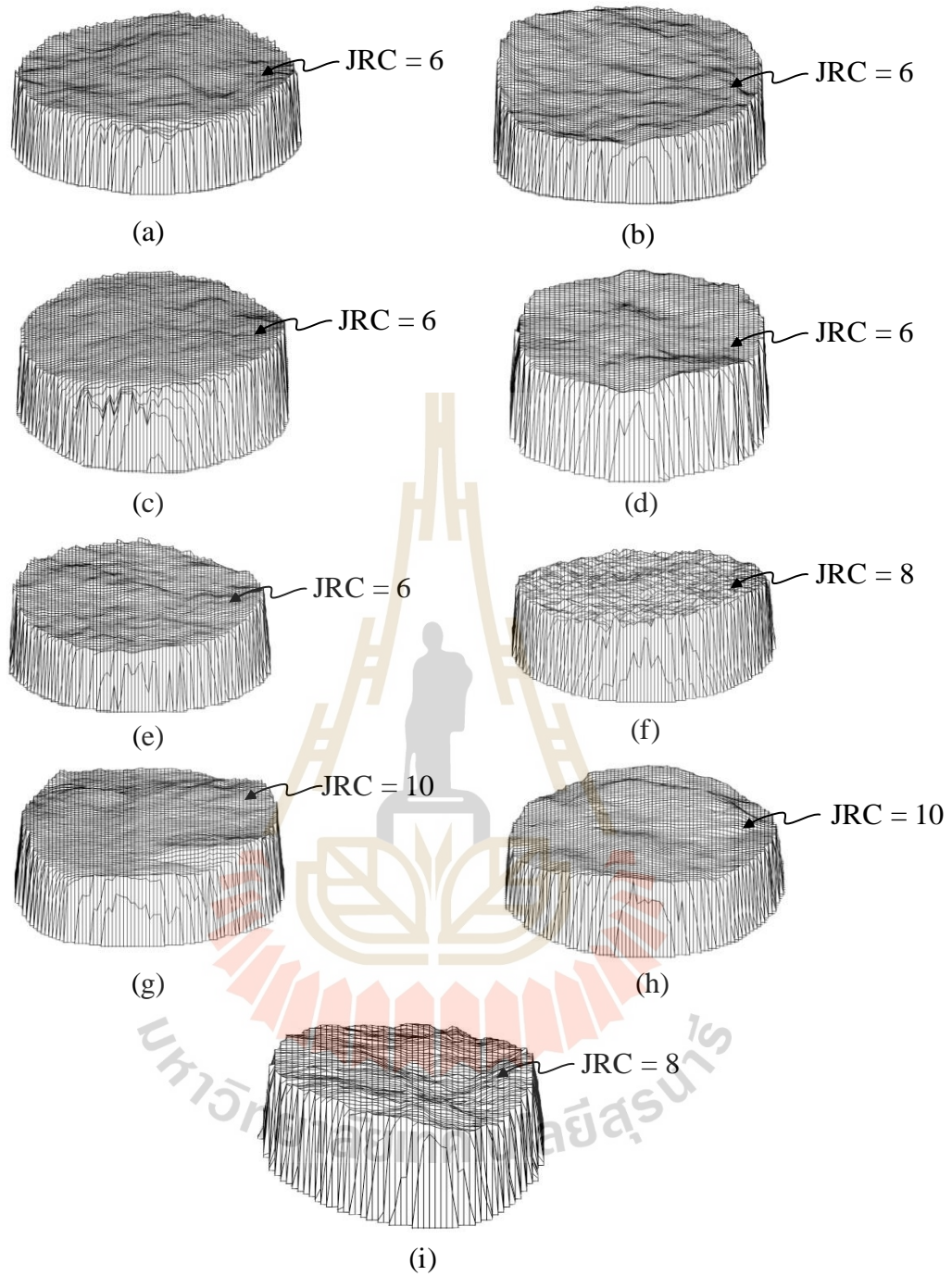


Figure 3.1 Representative laser scanned images of rough fracture for Phra Wihan sandstone (a), Sao Khua sandstone (b), Phu Tok sandstone (c), Phu Phan sandstone (d), Phu Kradung sandstone (e), Khao Khad marble (f), Khao Khad limestone (g), Khao Khad travertine (h), and Tak granite (i).

3.3 Sample preparation

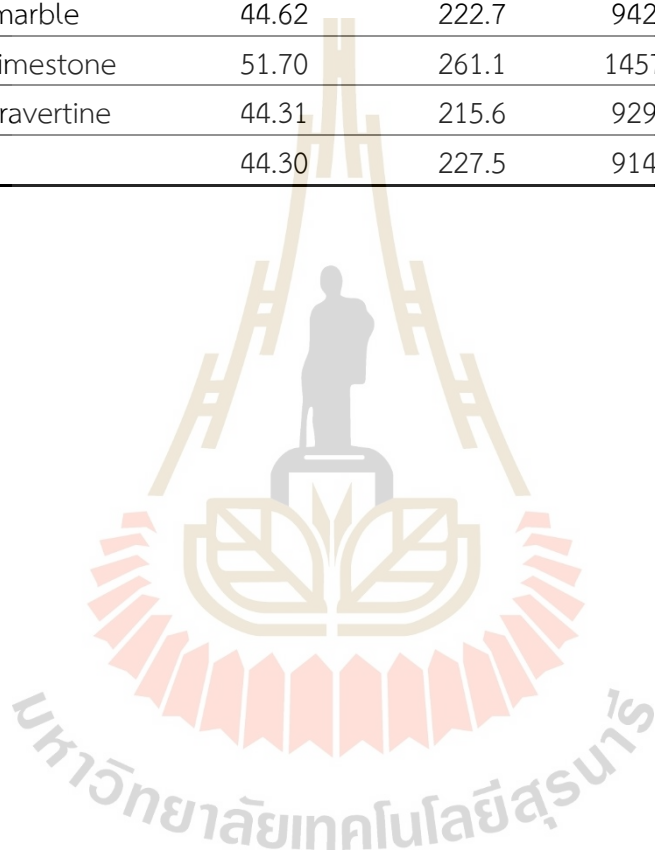
The specimens are prepared to obtain 45 mm in diameter and 225 mm in length with L/D ratio equal to 5. They are, prepared with bedding planes normal to the core axis (Figure 3.2). The specimens are tested under dry conditions. All of rock specimens have been prepared. Table 3.3 gives a summary of the physical properties of rock specimens including diameters, lengths, and weights. After preparation, all specimens are measured to obtain accurate length to calculate their specific gravity (SG) values. This method is carried out every time after the new fracture was created, then specific gravity of the specimens with different numbers of fractures is obtained.



Figure 3.2 Cylindrical specimens before fracture is induced. Phra Wihan sandstone (a), Sao Khua sandstone (b), Phu Tok sandstone (c), Phu Phan sandstone (d), Phu Kradung sandstone (e), Khao Khad marble (f), Khao Khad limestone (g), Khao Khad travertine (h), and Tak granite (i).

Table 3.3 Summary of physical properties of rock specimens.

Rock Types	Dimeter (mm)	Length (mm)	Weight (g)	Density (g/cc)
Phra Wihan sandstone	44.60	226.3	798.19	2.26
Sao Khua sandstone	51.60	268.1	1468.93	2.62
Phu Tok sandstone	44.32	224.0	837.57	2.42
Phu Phan sandstone	44.38	222.8	822.66	2.39
Phu Kradung sandstone	44.38	217.5	879.25	2.61
Khao Khad marble	44.62	222.7	942.51	2.71
Khao Khad limestone	51.70	261.1	1457.19	2.65
Khao Khad travertine	44.31	215.6	929.67	2.79
Tak granite	44.30	227.5	914.33	2.61



CHAPTER IV LABORATORY TESTING

4.1 Introduction

This chapter describes the methods of laboratory testing and calculations of the static loading tests and ultrasonic pulse velocity measurement as shown in Figure 4.1.

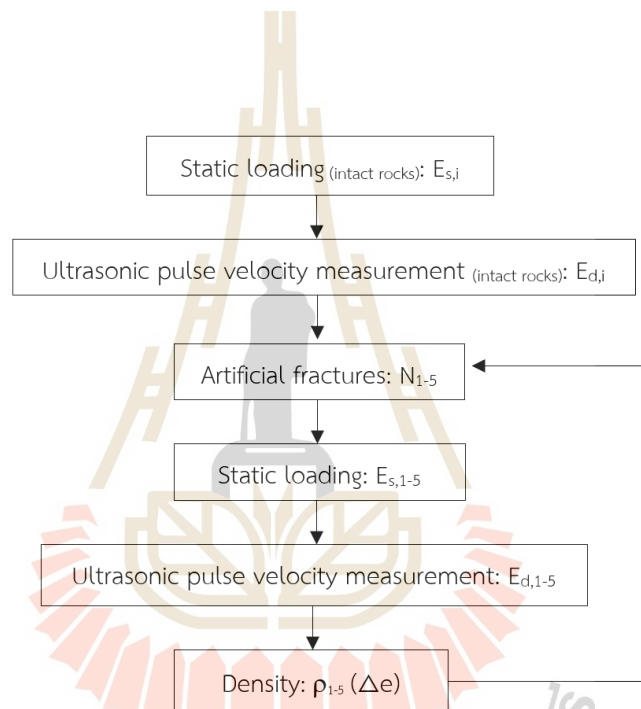


Figure 4.1 Methodology of laboratory testing.

4.2 Static loading

The static loading test follows the ASTM D7012-14 standard practice (Figure 4.2). Static loading method is performed on all rock samples to determine elastic modulus values (Elastic Static; E_s) each time before creating each artificial fracture. All artificial fractures are made by tension-inducing method (Figure 4.3). The fractures are normal to the core axis. Figure 4.4 show the specimens after all the fractures have been induced. The static loading test is performed by loading the specimen along its axis up to 10% of its strength as follows in Table 4.1. The Young's modulus of fractured specimens can be calculated by equation:

$$1/E_m = (N/K_n \cdot s) + (1/E_i) \quad (4.1)$$

where E_m is Young's modulus of fractured rock (GPa), E_i is the intact Young's modulus (GPa) which can be determined from static loading, s is joint spacing (m), N is equal to 1.0 for single joint set, and K_n is joint normal stiffness (GPa), determined by:

$$K_n = \sigma_{10\%} / \Delta e \quad (4.2)$$

where $\sigma_{10\%}$ is selected maximum stress at 10%, Δe is change of fracture aperture; Δe (mm) is determined before and after static loading to find the aperture of each fracture:

$$\Delta e = e_0 - e_1, \dots, e_5 \quad (4.3)$$

where e_0 is initial length and e_1, \dots, e_5 changed length of each artificial fracture.

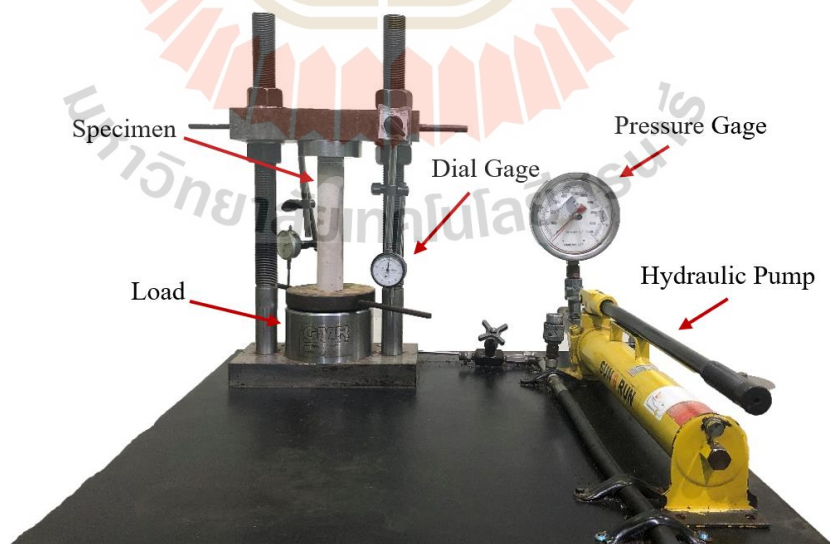


Figure 4.2 Uniaxial compression test device.



Figure 4.3 Creating an artificial fracture.

Table 4.1 Strength and maximum applied axial stress of each rock types.

Group	Rock Type	Strength (MPa)	Stress 10% (MPa)	Ref.
Clastic	Phra Wihan sandstone	70.4	2.21	Prasujan (2020)
	Sao Khua sandstone	52.4	2.20	
	Phu Phan sandstone	81.4	2.53	In this study
	Phu Kradung sandstone	80.1	2.49	
	Phu Tok sandstone	26.8	0.83	
Carbonate	Khao Khad marble	36.4	1.09	Chamwon (2021)
	Khao Khad limestone	77.3	2.27	
	Khao Khad travertine	59.6	1.85	
Plutonic	Tak granite	84.5	2.63	

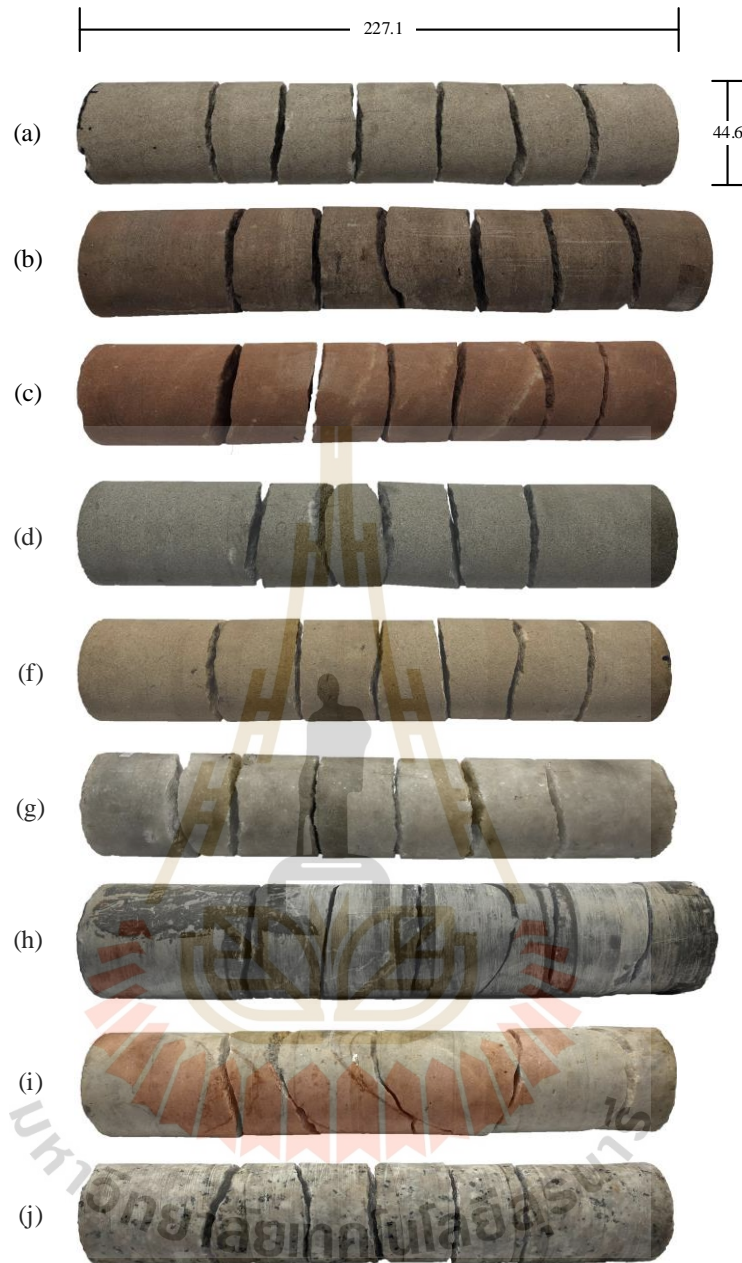


Figure 4.4 Core specimens after all fractures is induced Phra Wihan sandstone (a), Sao Khua sandstone (b), Phu Tok sandstone (c), Phu Phan sandstone (d), Phu Kradung sandstone (e), Khao Khad marble (f), Khao Khad limestone (g), Khao Khad travertine (h), and Tak granite (i).

4.3 Ultrasonic pulse velocity measurement

After the specimen is subjected to each static loading, the ultrasonic pulse velocity is measured in accordance with ASTM D2845-08 standard practice. OYO sonic

viewer (model 5378) with transmitter and receiver transducers is used with frequencies of 63 kHz for P-wave velocity and 53 kHz for S-wave velocity measurement (Figure 4.5). Thin film of silicone grease is applied on specimen end surfaces of coupling with the transducers. From the measured wave velocity and density, the dynamic deformation modulus (E_d) and Poisson's ratio (ν_d) for each intact and fractured rock specimen can be calculated as follows:

$$E_d = [\rho v_s^2 (3V_p^2 - 4v_s^2) / (V_p^2 - v_s^2)] \quad (4.4)$$

$$\nu_d = (V_p^2 - 2v_s^2) / 2(V_p^2 - v_s^2) \quad (4.5)$$

where V_p is P-wave velocity (km/s), V_s is S-wave velocity (km/s) and ρ is density for each rock type (g/cc) that calculated by:

$$\rho = W / (L + \Delta e) \cdot A \quad (4.5)$$

where W is weight of rock sample, L is length of rock sample, Δe is change of fracture aperture, and A is cross-sectional area of rock sample. Table 4.2 is shown the density for each rock type and after change of fractures are induced.



Figure 4.5 Some specimen of ultrasonic pulse velocity measurement.

Table 4.2 Density for each rock type and after change of fractures are induced.

Rock Type	Density (g/cc)					
	Intact	Fracture 1 st	Fracture 2 nd	Fracture 3 rd	Fracture 4 th	Fracture 5 th
Phra Wihan sandstone	2.2577	2.2538	2.2534	2.2531	2.2509	2.2495
Sao Khua sandstone	2.6201	2.6156	2.6136	2.6122	2.6111	2.6092
Phu Phan sandstone	2.4237	2.4234	2.4228	2.4225	2.4201	2.4185
Phu Kradung sandstone	2.3869	2.3852	2.3836	2.3829	2.3822	2.3803
Phu Tok sandstone	2.6138	2.6102	2.6078	2.6056	2.6016	2.6004
Khao Khad marble	2.7060	2.7025	2.7014	2.7011	2.6990	2.6963
Khao Khad limestone	2.6585	2.6578	2.6575	2.6566	2.6551	2.6538
Khao Khad travertine	2.7962	2.7949	2.7939	2.7932	2.7911	2.7893
Tak granite	2.6075	2.6067	2.6063	2.6060	2.6042	2.6028

CHAPTER V

TEST RESULTS

5.1 Introduction

This chapter describes the results of laboratory testing of the static loading tests and ultrasonic pulse velocity measurements. The results of static loading test determine parameters such as change of fracture aperture (Δe) and joint normal stiffness (K_n) to calculate Young's modulus of fractured rock (E_m) of each rock type. Ultrasonic pulse velocity measurement testing measures P and S-wave velocities (km/s) to calculate dynamic deformation modulus (E_d) and Poisson's ratio (ν_d).

5.2 Static loading tests

Static loading tests are performed under dry condition to determine the Young's modulus of fractured rock specimens (E_m). The testing uses the maximum applied axial stress of each rock type with 5 cycles of loading-unloading. The calculated tangent Young's moduli of fractured rock ($E_{m,m}$) are averaged from 5 tangent lines of reloading curves and calculate Young's moduli of fractured rock ($E_{m,c}$) using equation (4.1). The results are shown in Figures 5.1 to 5.9 and Table 5.1. The linear relationship shows the change of fracture aperture (Δe) between number of apertures with number of fractures, as shown in Figure 5.10. The linear relationship between joint normal stiffness (K_n) and number of fractures are shown in Figure 5.11. The relationship between $E_{m,m}$ and $E_{m,c}$ with the number of fractures shows that both Young's moduli of fractured rock ($E_{m,m}$ and $E_{m,c}$) is affected by increasing number of fractures. The linear relations show $R^2 = 0.9$, as shown in Figures 5.12 to 5.13. The relationship between $E_{m,m}$ and $E_{m,c}$ (Figure 5.14) shows that $E_{m,m}$ has good correlations with $E_{m,c}$ by linear relation for all rock types and gives $R^2 = 0.923$.

The largest $E_{m,m}$ and $E_{m,c}$ values are obtained from Tak granite, while the smallest ones are from Phu Tok sandstone. The sandstone tends to show the higher values of $E_{m,m}$ and $E_{m,c}$ than those of marble and travertine. (Figures 5.12 and 5.13).

For all rock types, strong correlation is obtained between $E_{m,m}$ and $E_{m,c}$ as shown in Figure 5.14. This suggests that increasing the number of fractures tends to show similar effect on both static and dynamic Young's moduli.

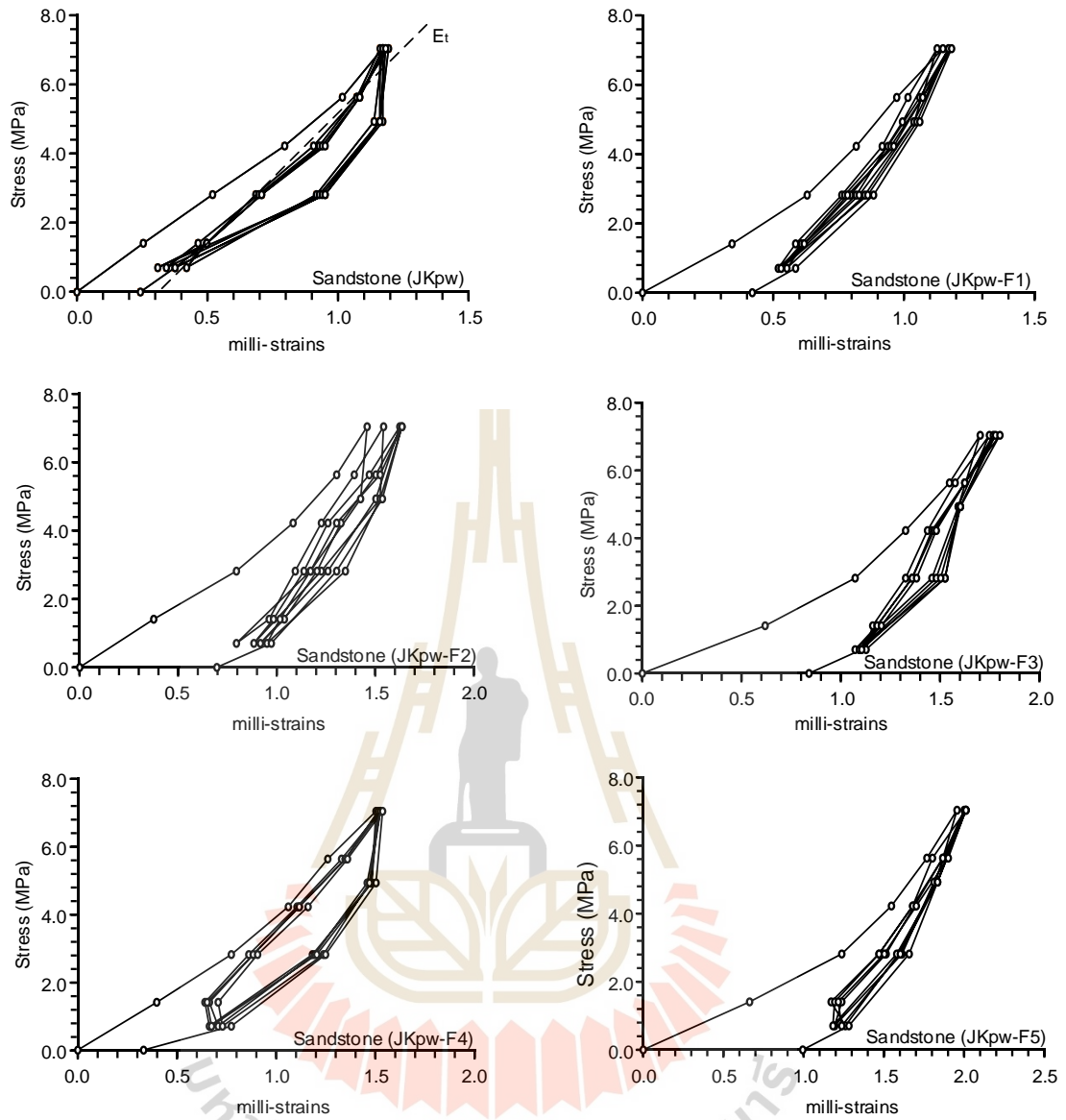


Figure 5.1 Static loading test results of each fracture for Phra Wihan sandstone.

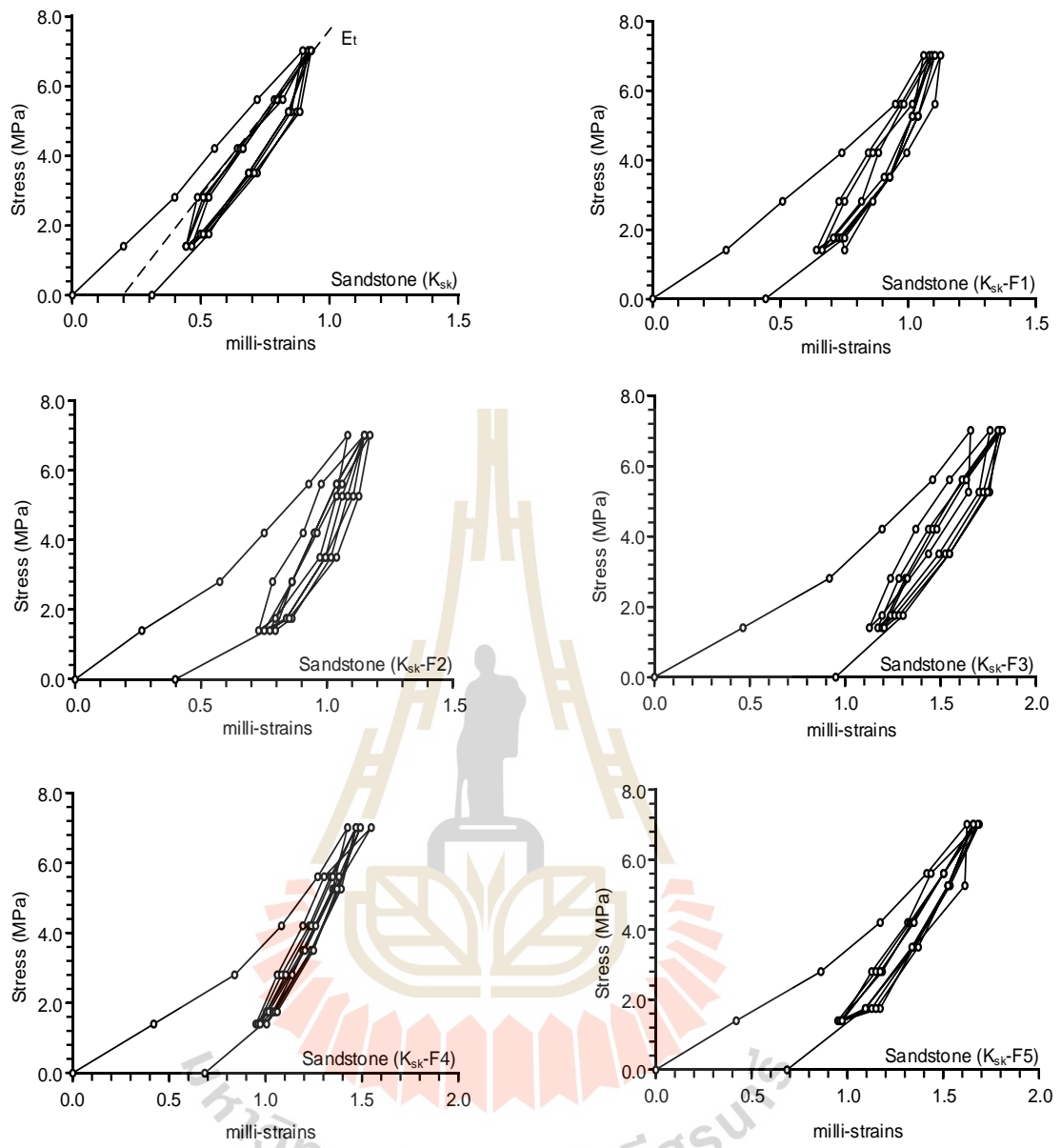


Figure 5.2 Static loading test results of each fracture for Sao Khua sandstone.

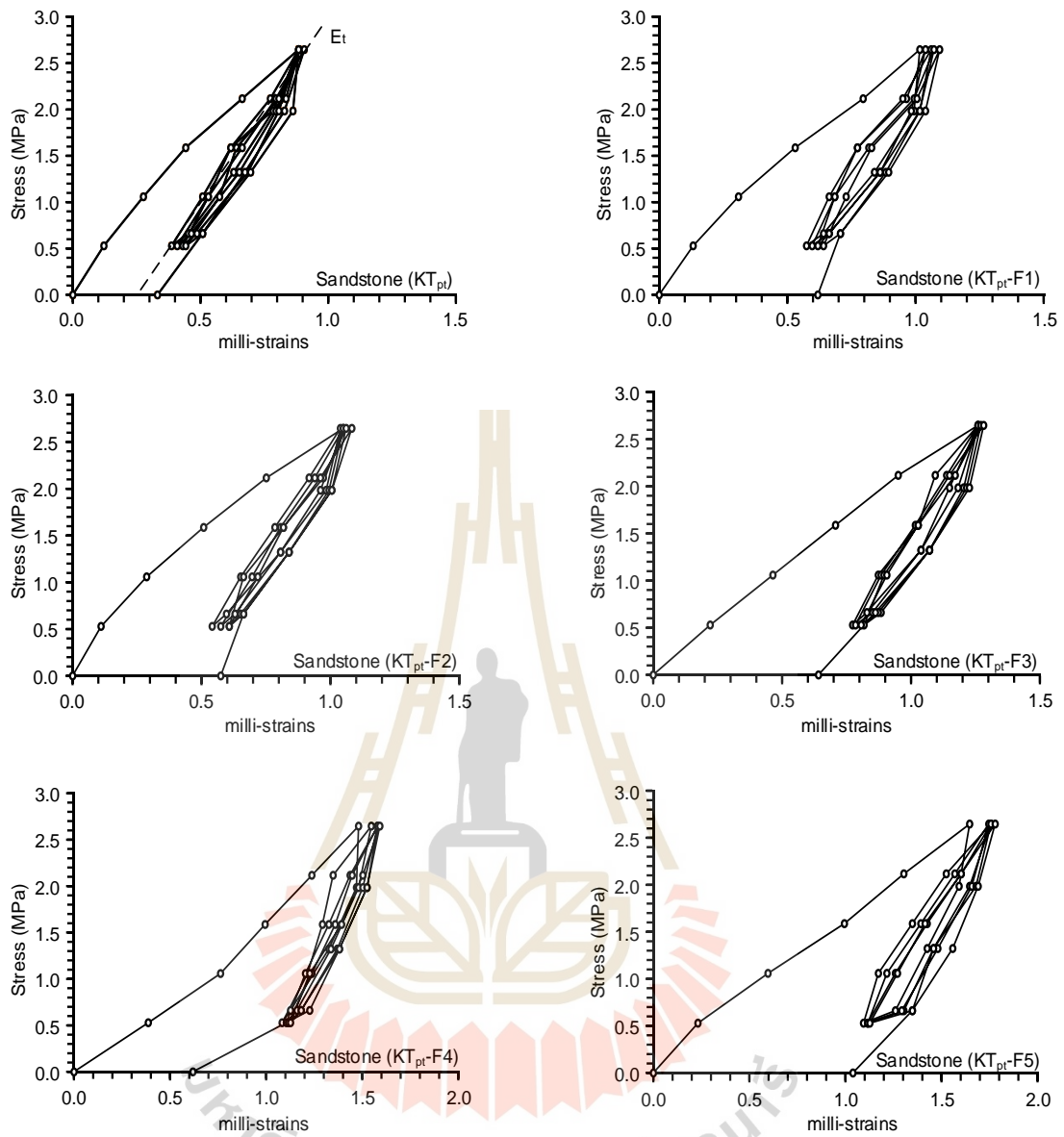


Figure 5.3 Static loading tests result of each fracture for Phu Tok sandstone.

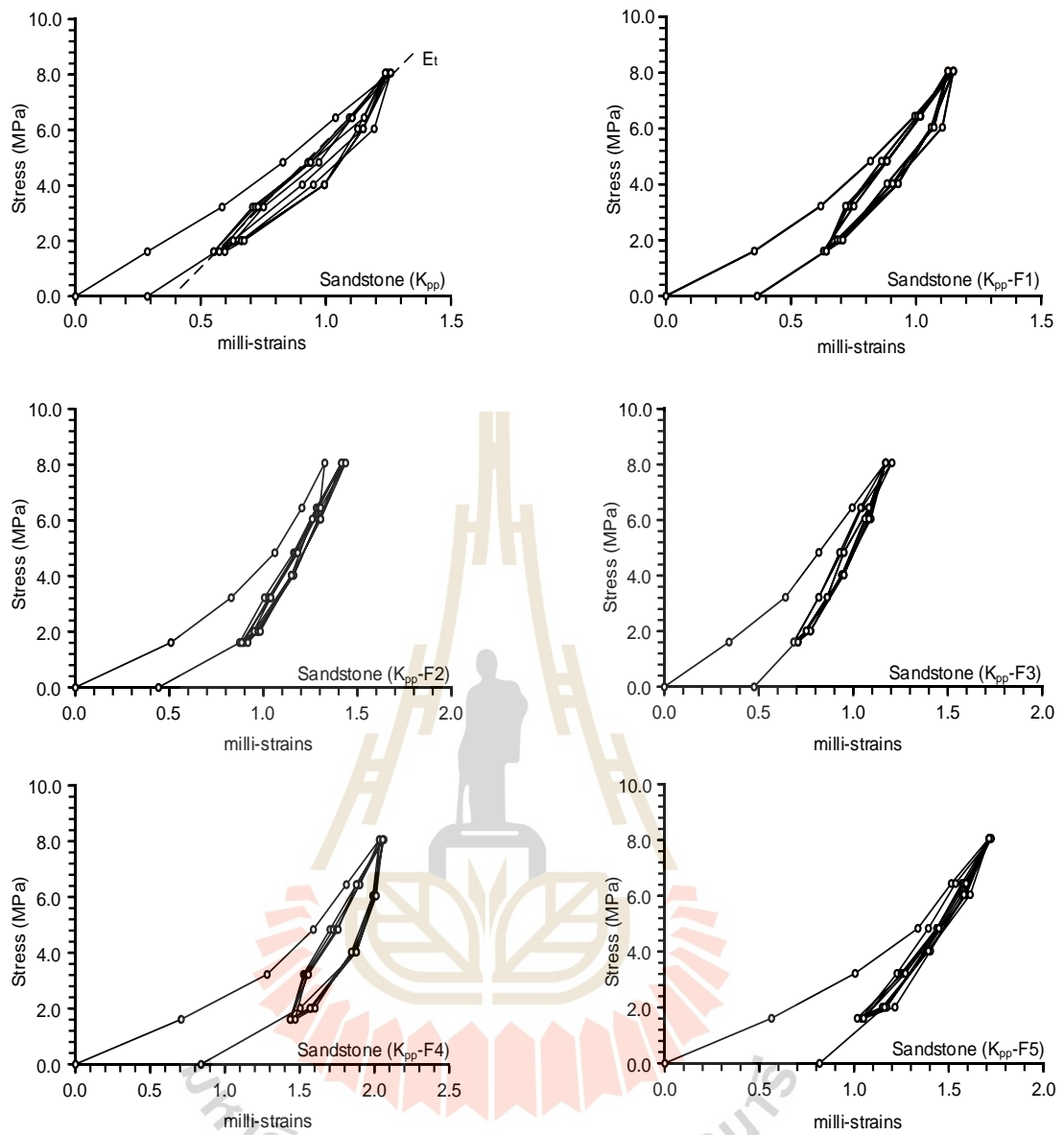


Figure 5.4 Static loading test results of each fracture for Phu Phan sandstone.

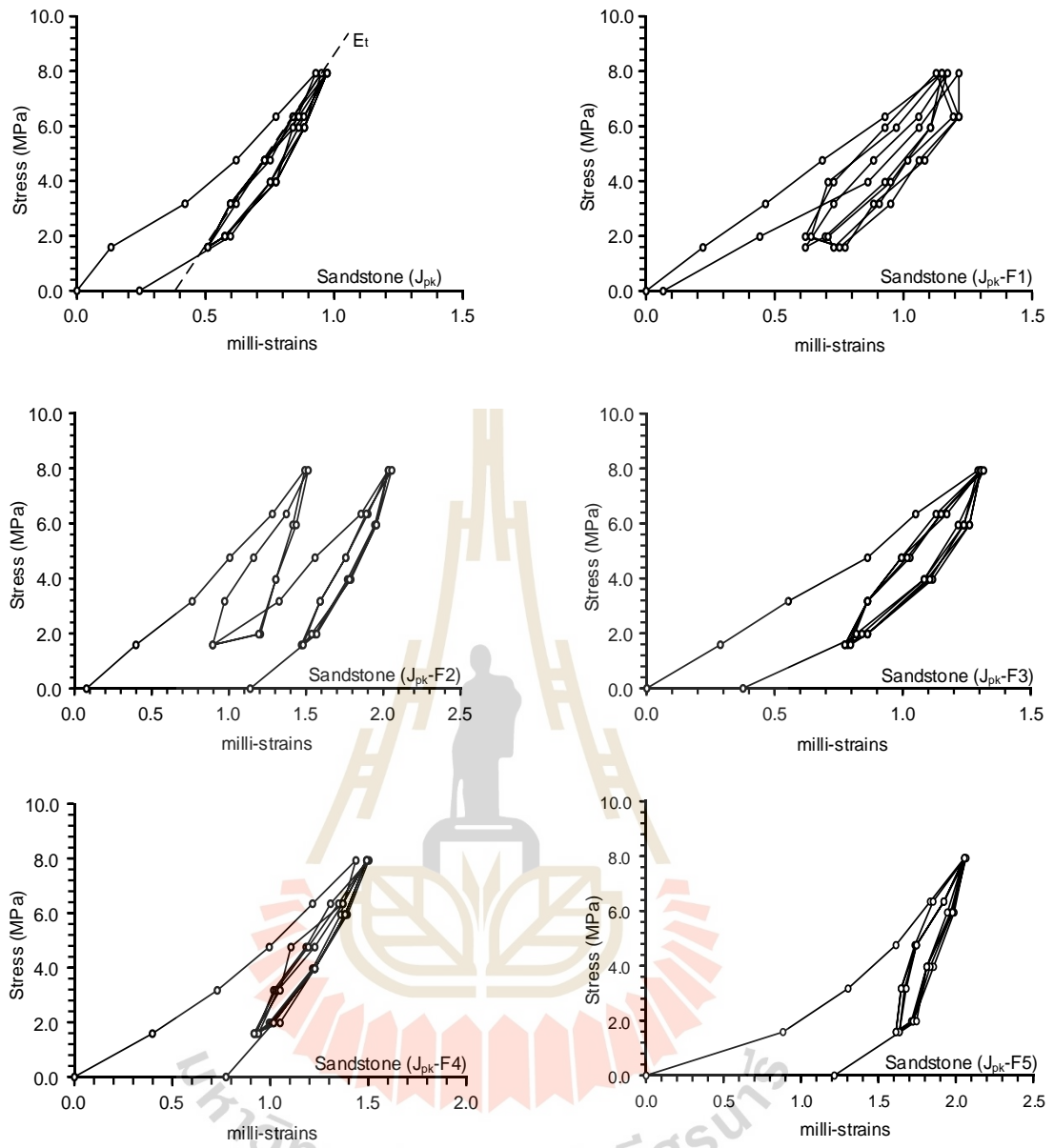


Figure 5.5 Static loading test results of each fracture for Phu Krading sandstone.

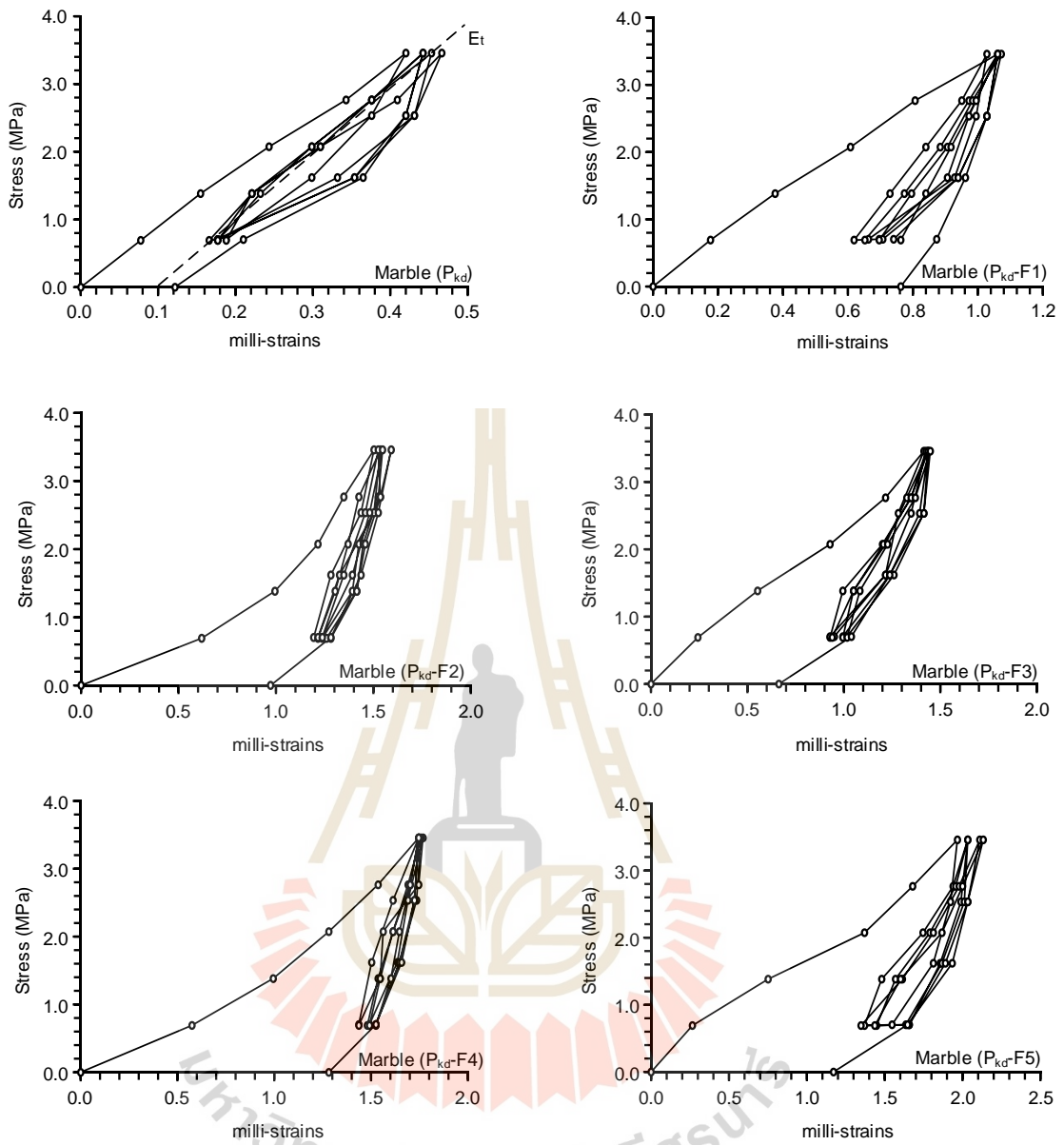


Figure 5.6 Static loading tests result of each fracture for Khao Khad marble.

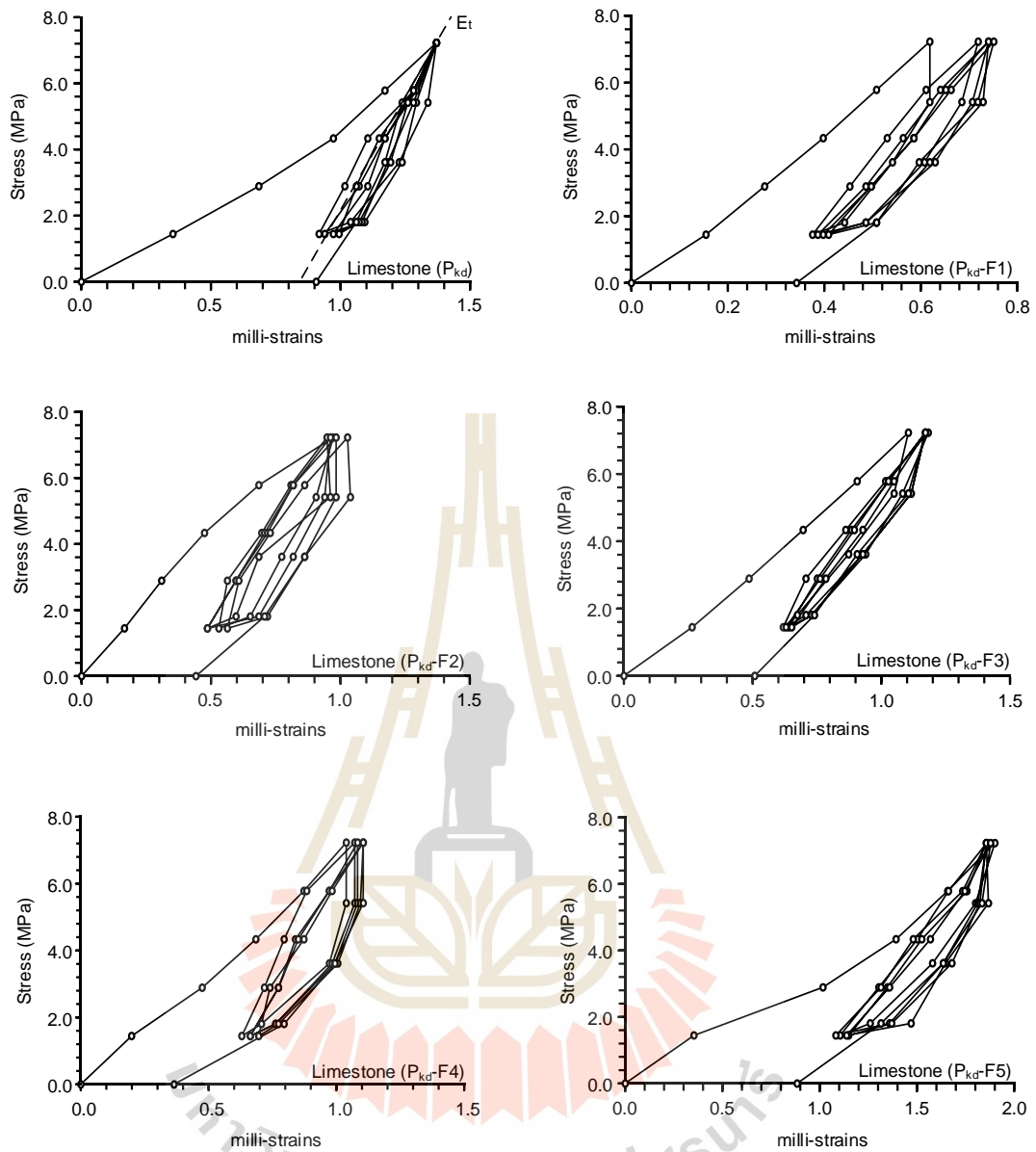


Figure 5.7 Static loading test results of each fracture for Khao Khad limestone.

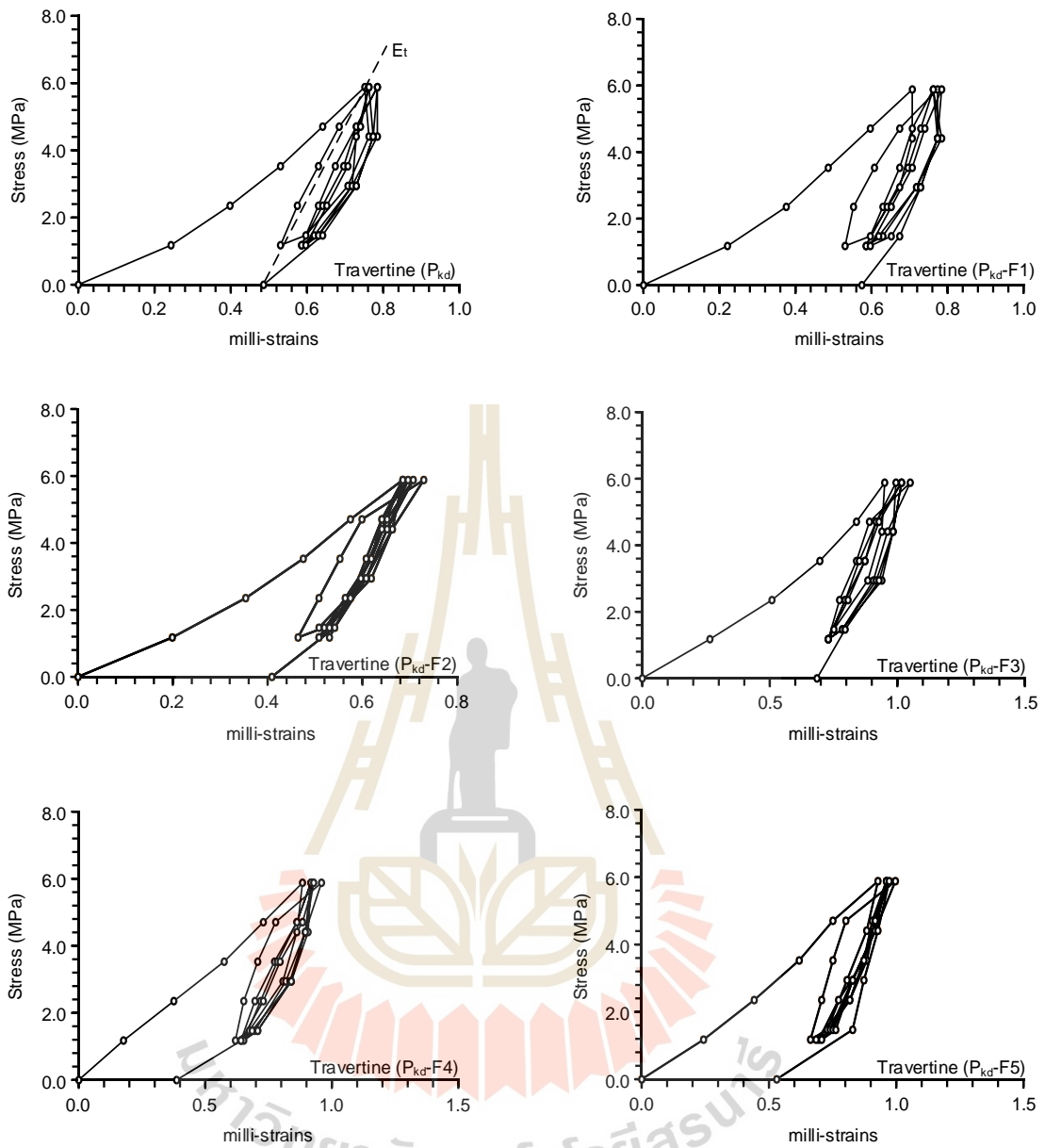


Figure 5.8 Static loading test results of each fracture for Khao Khad travertine.

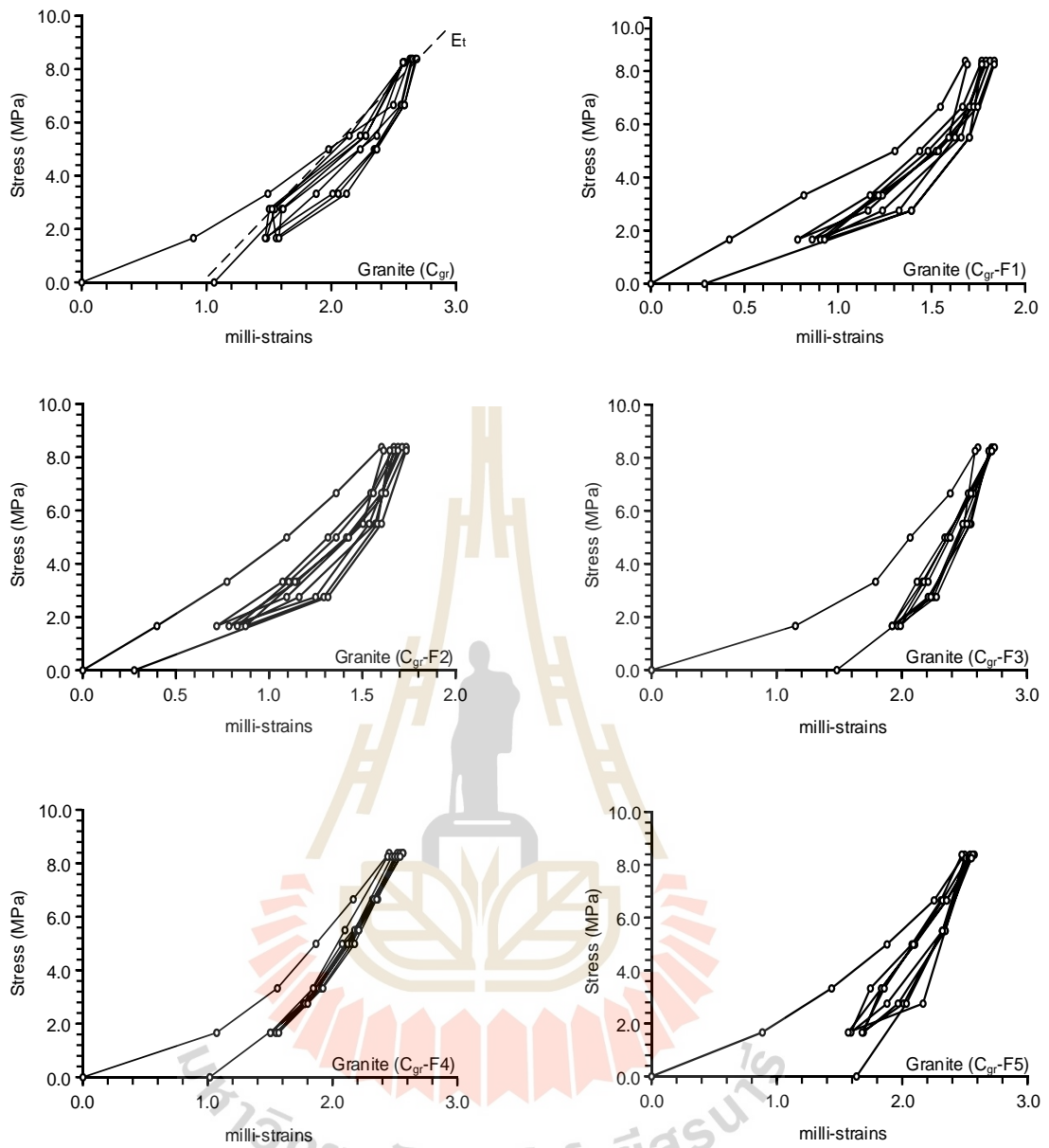


Figure 5.9 Static loading test results of each fracture for Tak granite.

Table 5.1 Summary of physical and mechanical properties of rock specimens measured under static loading.

Number of fractures	Rock type	Δe	K_n (GPa)	s (mm)	$E_{m,m}$ (GPa)	$E_{m,c}$ (GPa)
0	Phra Wihan sandstone	0	-	226.76	15.90	15.90
1		0.222	9.96	113.38	12.62	13.94
2		0.256	8.65	75.59	9.48	12.79
3		0.298	7.42	56.69	8.17	11.54
4		0.355	6.23	45.35	7.20	10.17
5		0.411	5.39	37.79	6.76	8.93
0	Sao Khua sandstone	0	-	266.10	14.11	14.11
1		0.314	7.02	133.05	10.94	12.25
2		0.359	6.13	88.70	8.19	11.20
3		0.447	4.93	66.53	6.59	9.86
4		0.530	4.16	53.22	5.75	8.62
5		0.603	3.66	44.35	5.58	7.54
0	Phu Tok sandstone	0	-	224.00	10.13	10.13
1		0.190	4.38	112.00	7.15	8.39
2		0.253	3.29	74.67	4.35	7.17
3		0.305	2.73	56.00	3.19	6.09
4		0.338	2.46	44.80	2.64	5.28
5		0.400	2.08	37.33	2.28	4.40
0	Phu Phan sandstone	0	-	222.80	18.43	18.43
1		0.187	13.54	111.40	14.89	16.43
2		0.207	12.22	74.27	12.06	15.32
3		0.241	10.51	55.70	10.16	14.02
4		0.303	8.36	44.56	8.80	12.33
5		0.360	7.04	37.13	8.61	10.81
0	Phu Kradung sandstone	0	-	217.46	17.51	17.51
1		0.200	12.46	108.73	14.18	15.50
2		0.230	10.83	72.49	11.21	14.31
3		0.268	9.31	54.37	9.09	13.01
4		0.320	7.79	43.49	8.11	11.54
5		0.390	6.39	36.24	7.64	9.97

Table 5.1 Summary of physical and mechanical properties of rock specimens measured under static loading. (Cont.)

Number of fractures	Rock type	Δe	K_n (GPa)	s (mm)	$E_{m,m}$ (GPa)	$E_{m,c}$ (GPa)
0	Khao Khad marble	0	-	223.16	12.03	12.03
1		0.200	5.43	111.58	8.94	10.04
2		0.242	4.49	74.39	6.26	8.84
3		0.285	3.81	55.79	4.65	7.68
4		0.330	3.29	44.63	3.77	6.61
5		0.389	2.79	37.19	3.57	5.57
0	Khao Khad limestone	0	-	261.30	16.69	16.69
1		0.199	11.41	130.65	13.38	15.01
2		0.231	9.83	87.10	10.38	13.97
3		0.274	8.29	65.33	8.72	12.76
4		0.319	7.12	52.26	7.70	11.52
5		0.385	5.90	43.55	7.35	10.12
0	Khao Khad travertine	0	-	215.61	15.08	15.08
1		0.226	8.19	107.81	11.80	12.88
2		0.277	6.67	71.87	9.02	11.47
3		0.327	5.64	53.90	7.35	10.08
4		0.393	4.70	43.12	6.49	8.65
5		0.439	4.21	35.94	6.05	7.55
0	Tak granite	0	-	227.63	20.42	20.42
1		0.170	15.49	113.82	16.92	18.30
2		0.198	13.34	75.88	13.91	16.99
3		0.230	11.45	56.91	11.94	15.55
4		0.285	9.24	45.53	10.74	13.75
5		0.345	7.63	37.94	10.36	11.98

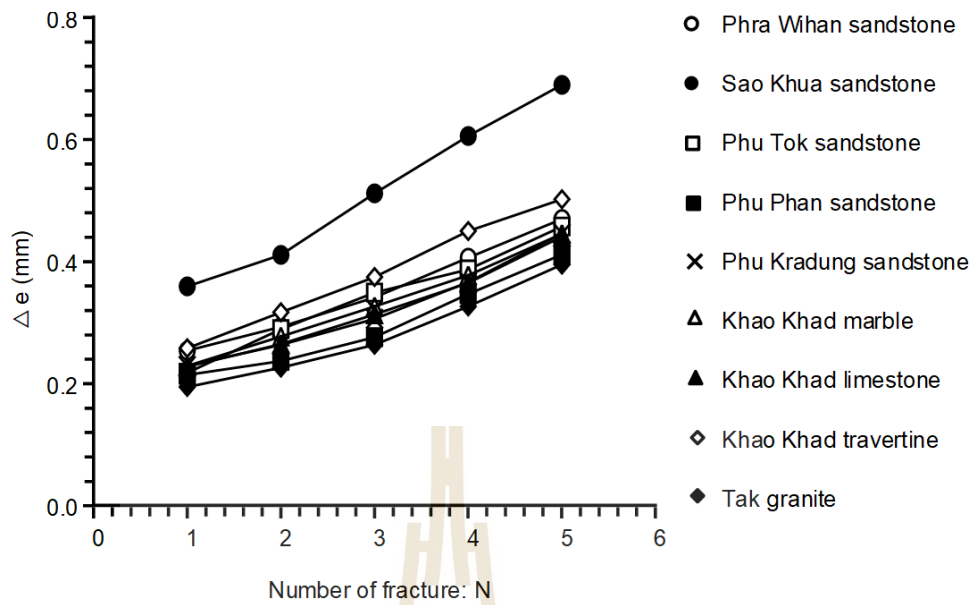


Figure 5.10 Relationship between change of fracture aperture (Δe) and number of fractures.

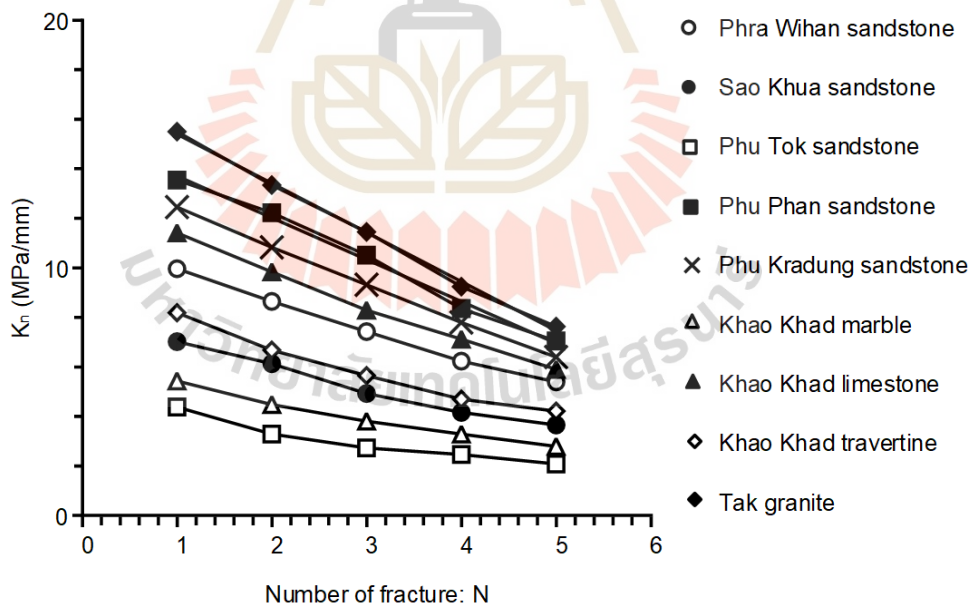


Figure 5.11 Relationship between joint normal stiffness (K_n) and number of fractures.

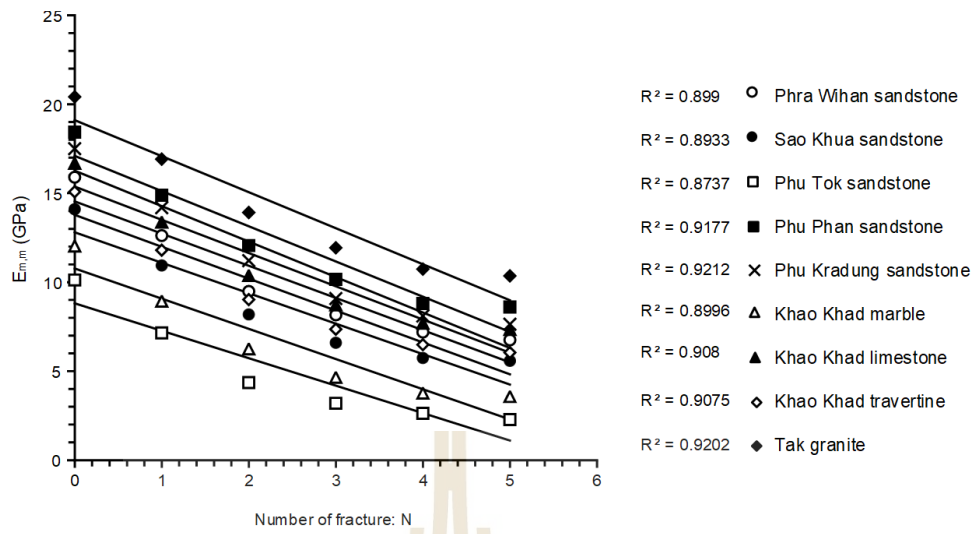


Figure 5.12 Relationship between Young's moduli of fractured rock: $E_{m,m}$ and number of fractures.

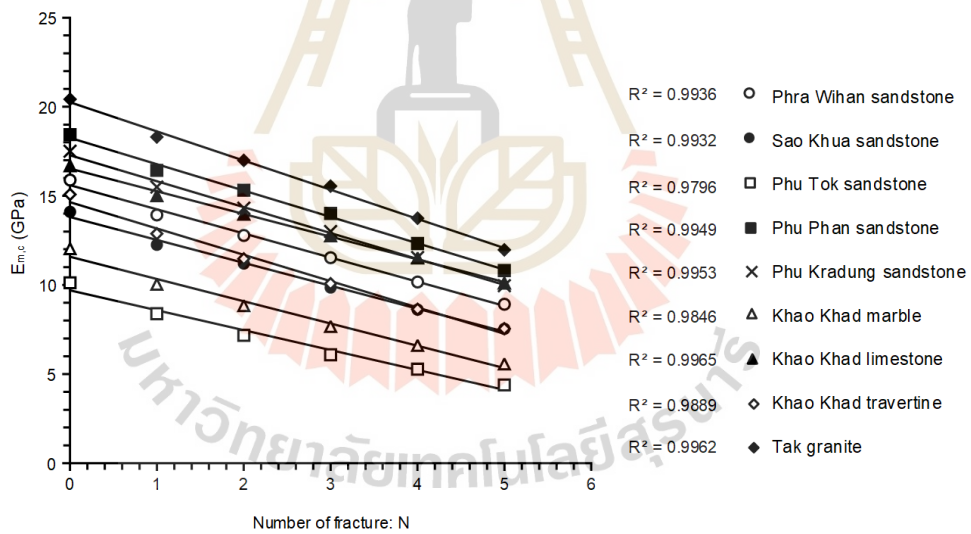


Figure 5.13 Relationship between Young's moduli of fractured rock: $E_{m,c}$ and number of fractures.

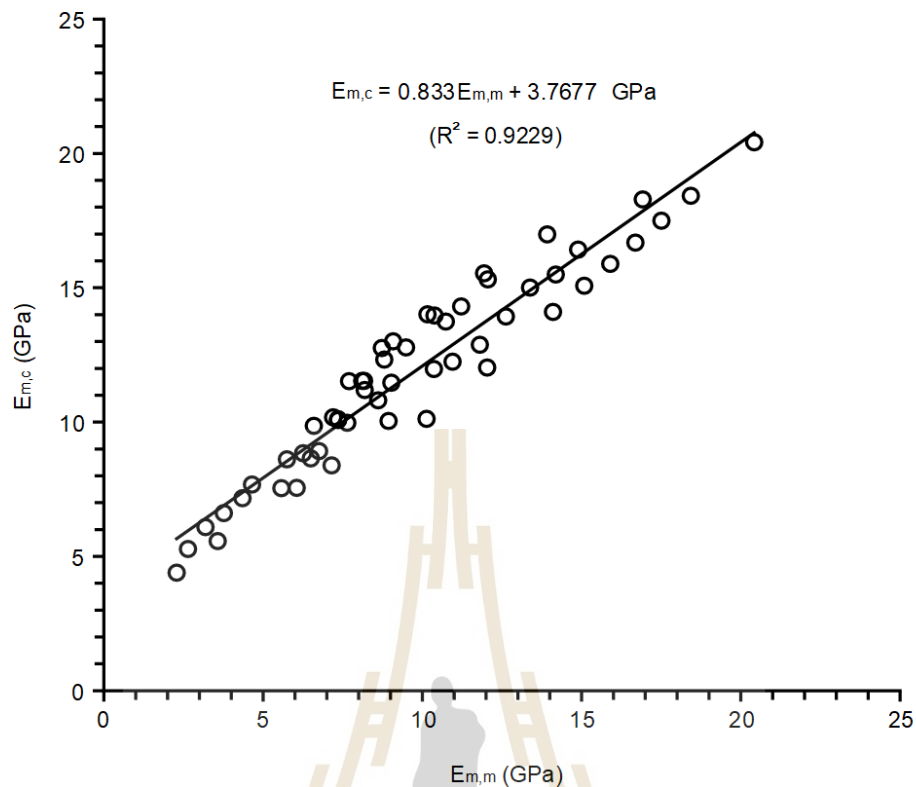


Figure 5.14 Relationship between Young's moduli of fractured rock: $E_{m,m}$ and Young's moduli of fractured rock: $E_{m,c}$.

5.3 Ultrasonic pulse velocity (UPV) measurement tests

UPV measurements are performed for every increasing number of fractures for each rock type. The dynamic deformation modulus (E_d) and Poisson's ratio (ν_d) are calculated by measuring P and S-wave velocities (km/s) using equations (4.4) and (4.5). The results are given in Table 5.2. The linear relationship between P-wave velocity and S-wave velocity and number of fractures is obtained. The differences of density are calculated by equation (4.6) for increasing number of fractures. P and S-waves correlate well with the number of fractures as shown in Figures 5.15 and 5.16.

Table 5.2 Summary of physical properties of rock specimens for UPV measurements.

Number of fractures	Rock type	V_p (km/s)	V_s (km/s)	E_d (GPa)	v_d	Density (g/cc)
0	Phra Wihan sandstone	3.836	2.286	28.893	0.225	2.258
1		3.383	2.061	23.098	0.205	2.254
2		2.945	1.828	17.873	0.186	2.253
3		2.492	1.608	13.322	0.143	2.253
4		2.063	1.359	9.288	0.117	2.251
5		1.788	1.202	7.071	0.088	2.249
0	Sao Khua sandstone	3.310	2.001	25.426	0.212	2.620
1		2.857	1.767	19.439	0.190	2.616
2		2.421	1.554	14.510	0.150	2.614
3		2.007	1.325	10.212	0.114	2.612
4		1.630	1.103	6.843	0.079	2.611
5		1.276	0.883	4.233	0.041	2.609
0	Phu Tok sandstone	3.111	1.723	18.404	0.279	2.614
1		2.489	1.484	13.064	0.225	2.610
2		2.037	1.245	9.024	0.202	2.608
3		1.624	1.028	5.969	0.166	2.606
4		1.150	0.743	3.050	0.142	2.602
5		0.741	0.496	1.301	0.095	2.601
1		3.596	2.208	27.843	0.198	2.423
2		3.234	2.066	23.502	0.155	2.423
3		2.790	1.860	18.133	0.100	2.423
4		2.453	1.666	14.165	0.072	2.420
5		2.212	1.530	11.606	0.041	2.419
0	Phu Kradung sandstone	3.842	2.265	33.089	0.234	2.387
1		3.350	2.035	26.110	0.208	2.385
2		3.027	1.895	22.064	0.178	2.384
3		2.566	1.678	16.531	0.127	2.383
4		2.207	1.496	12.513	0.074	2.382
5		1.969	1.349	10.013	0.058	2.380

Table 5.2 Summary of physical properties of rock specimens for UPV measurements.
(Cont.).

Number of fractures	Rock type	V_p (km/s)	V_s (km/s)	E_d (GPa)	ν_d	Density (g/cc)
0	Khao Khad marble	2.720	1.628	17.491	0.221	2.706
1		2.254	1.386	12.412	0.196	2.703
2		1.800	1.156	8.295	0.149	2.702
3		1.423	0.946	5.327	0.103	2.701
4		1.065	0.717	3.006	0.086	2.699
5		2.720	1.628	17.491	0.221	2.696
0	Khao Khad limestone	3.677	2.176	30.979	0.231	2.659
1		3.225	1.994	25.156	0.191	2.658
2		2.808	1.765	19.430	0.174	2.657
3		2.441	1.574	15.062	0.145	2.656
4		2.108	1.398	11.491	0.108	2.655
5		1.804	1.217	8.506	0.083	2.654
0	Khao Khad travertine	3.654	1.978	27.066	0.237	2.796
1		2.996	1.768	21.126	0.209	2.795
2		2.539	1.564	15.988	0.170	2.794
3		2.225	1.349	11.531	0.134	2.793
4		1.964	1.174	8.516	0.108	2.791
5		1.772	0.956	5.495	0.077	2.789
0	Tak granite	4.136	2.556	40.586	0.191	2.608
1		3.793	2.370	34.554	0.179	2.607
2		3.397	2.210	28.845	0.133	2.606
3		3.076	2.032	23.954	0.113	2.606
4		2.812	1.883	20.183	0.094	2.604
5		2.590	1.753	17.233	0.077	2.603

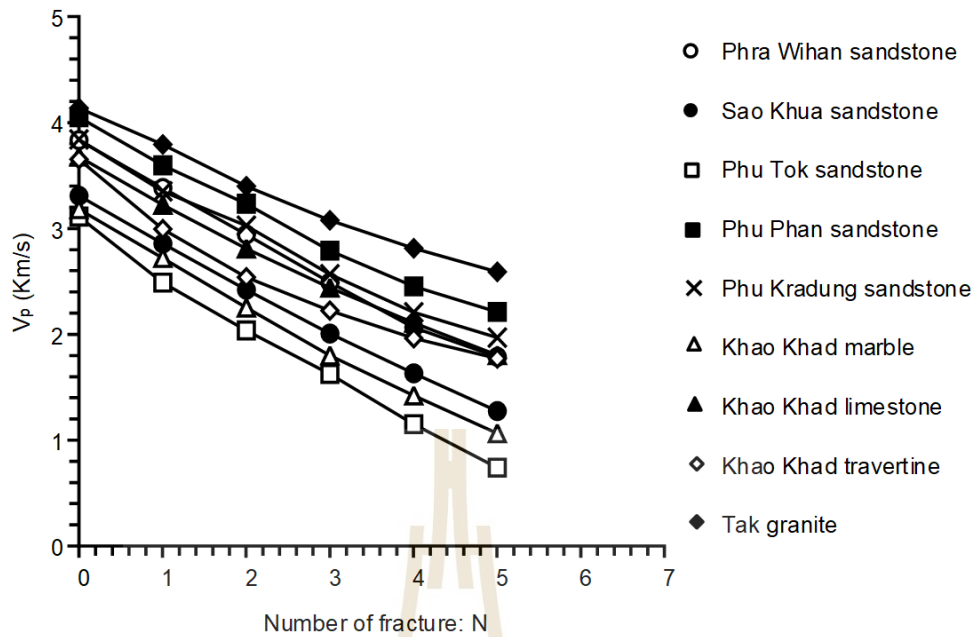


Figure 5.15 Relationship between P-wave velocity (km/s) and number of fractures.

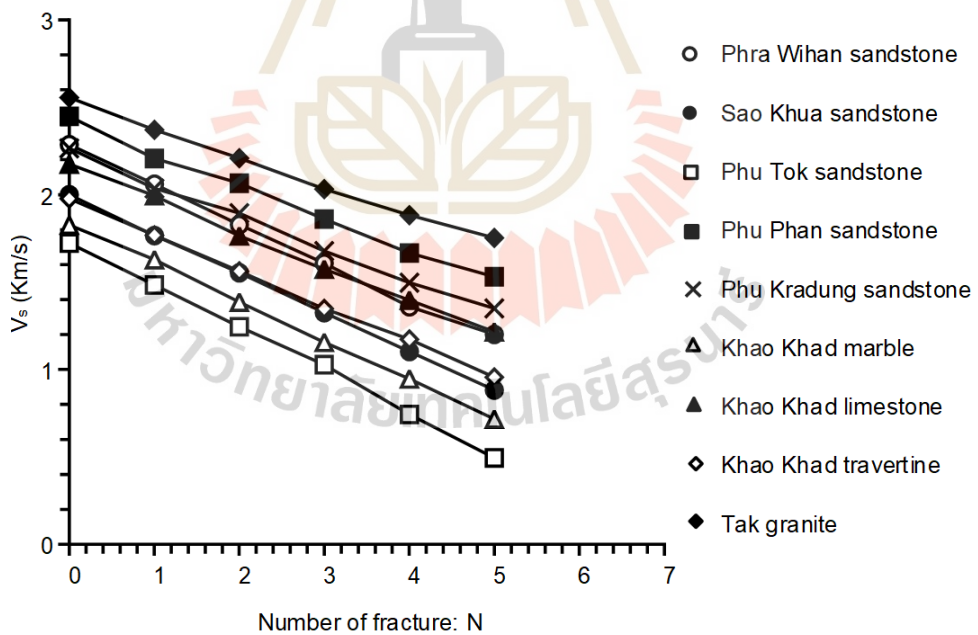


Figure 5.16 Relationship between S-wave velocity (km/s) and number of fractures.

CHAPTER VI

RELATIONSHIP BETWEEN STATIC AND DYNAMIC PARAMETER

6.1 Introduction

This chapter describes the development of the mathematical relationship between dynamic deformation modulus (E_d) and static deformation modulus (E_s) obtained from the test results in chapter V. The results can be useful to predict the static parameters from the dynamic parameters of rock mass.

6.2 Dynamic deformation modulus

The relationship between dynamic deformation modulus and the number of fractures shows the decrease of the dynamic parameter by the increase of the number of fractures. Dynamic modulus is varied among different rock types, as shown in Figure 6.1. The test results can be represented by polynomial equation:

$$E_d = E_{d,i} - NB + NC^2 \quad (6.1)$$

where $E_{d,i}$ is dynamic modulus for intact rock, B is slope of polynomial equation, C is curvature of polynomial equation which tends to be constant equal to 0.41, and N is number of fractures. Table 6.1 gives parameters for different slope values, which varies with ascending dynamic deformation modulus of each intact rock.

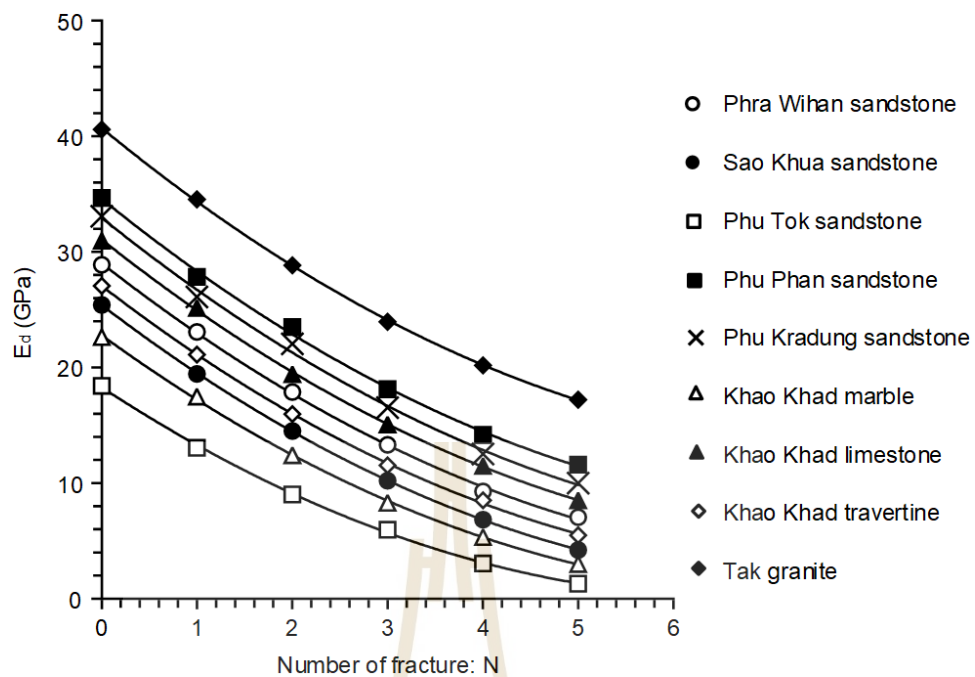


Figure 6.1 Relationship between dynamic deformation modulus (E_d) and number of fractures.

Table 6.1 Parameters of polynomial equation for dynamic deformation modulus of each rock type.

Rock Type	B	C	$E_{d,i}$ (GPa)
Phu Tok sandstone	5.3924	0.4007	18.4
Khao Khad marble	5.9797	0.4030	22.6
Sao Khua sandstone	6.2945	0.4129	25.4
Khao Khad travertine	6.3514	0.4123	27.1
Phra Wihan sandstone	6.4536	0.4045	28.9
Khao Khad limestone	6.543	0.4073	31.0
Phu Kradung sandstone	6.6298	0.4019	33.1
Phu Phan sandstone	6.6712	0.4096	34.7
Tak granite	6.7757	0.4136	40.6

6.3 Static deformation modulus

Relationship between static deformation modulus and number of fractures can be developed, as shown in Figure 6.2. The number of fractures affects the static

deformation modulus less than the dynamic deformation modulus. The relationship can be established by the polynomial equation:

$$E_s = E_{s,i} - ND + NF^2 \quad (6.2)$$

where $E_{s,i}$ is obtained from intact rock, D is slope of polynomial equation, F is curvature of polynomial equation which tends to be constant value equal to 0.41, and N is number of fractures. Table 6.2 gives the parameters for the proposed polynomial equation.

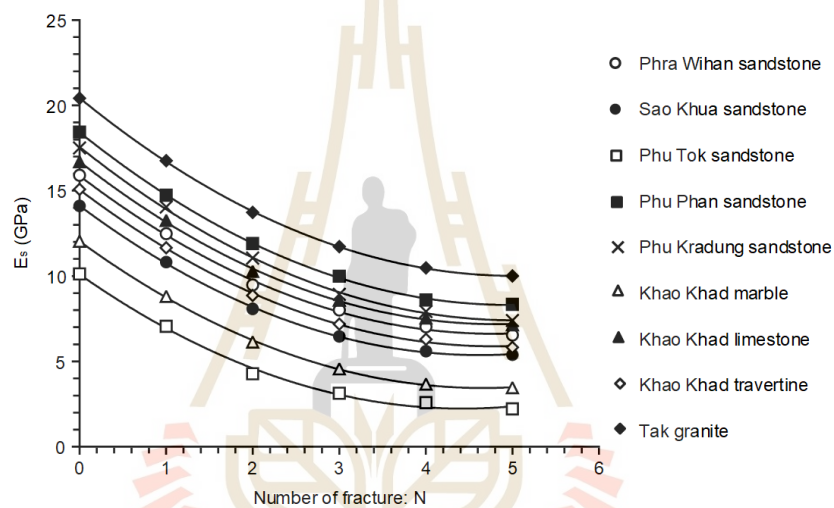


Figure 6.2 Relationship between static deformation modulus (E_s) and number of fractures.

Table 6.2 Parameters of polynomial equation for static deformation modulus of each rock type.

Rock Type	D	F	$E_{s,i}$ (GPa)
Phu Tok sandstone	3.5522	0.4012	10.1
Khao Khad marble	3.6895	0.3959	12.0
Sao Khua sandstone	3.7853	0.4096	14.1
Khao Khad travertine	3.8313	0.4001	15.1
Phra Wihan sandstone	3.874	0.4155	15.9
Khao Khad limestone	3.9548	0.4107	16.7
Phu Kradung sandstone	4.0482	0.4036	17.5
Phu Phan sandstone	4.0745	0.4103	18.4
Tak granite	4.1434	0.4118	20.4

6.4 Relationship of slope values of polynomial equation

The slope values of dynamic and static deformation moduli are varied with joint normal stiffness (K_n) which can be represented by a linear relationship:

$$B = 0.1014K_n + 5.353 \quad (6.3)$$

$$D = 0.05K_n + 3.3954 \quad (6.4)$$

where B is slope value of dynamic deformation modulus, D is slope value of static deformation modulus, and K_n is joint normal stiffness. Figure 6.3 shows the comparison slopes values B and D as a function of joint normal stiffness. The results show that the slope of dynamic deformation modulus (E_d) is higher than that of the static deformation modulus (E_s). Figure 6.4 shows the relation between slopes B and D from polynomial equation of all rock types which can be represented by a linear relationship:

$$D = 0.4261B + 1.1806 \quad (6.5)$$

where D is slope of polynomial equation of static deformation modulus, B is slope of polynomial equation of dynamic deformation modulus. This equation shows good correlation ($R^2 = 0.890$).

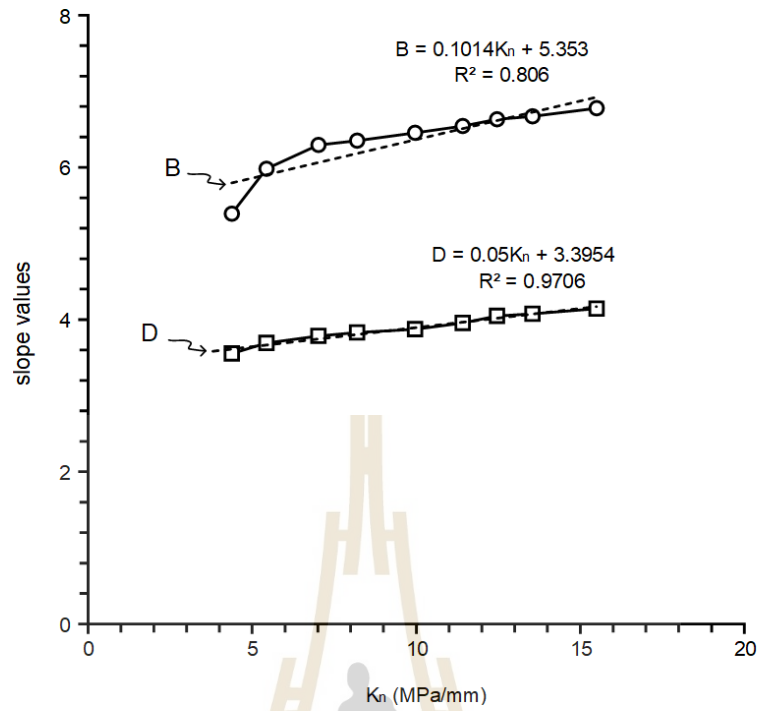


Figure 6.3 Slopes B (dynamic deformation modulus) and D (static deformation modulus) as a function of joint normal stiffness (K_n).

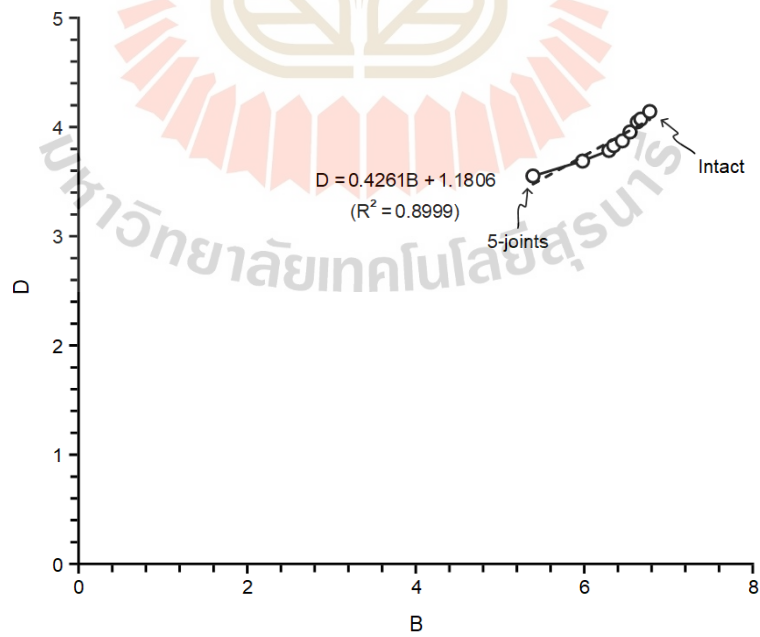


Figure 6.4 Relationship between slope B (Dynamic deformation modulus, E_d) and D (Static deformation modulus, E_s)

6.5 Correlations between dynamic and static deformation moduli

The decreases of the dynamic and static deformation moduli can be correlated with number of fractures. All rock types have a similar trend showing linear relationship:

$$E_s = XE_d + Y \quad (6.6)$$

where E_s is dynamic deformation modulus, X is slope of linear equation of each rock type, E_d is static deformation modulus, and Y is material constant depending on rock type. Table 6.3 gives the parameters for prediction static deformation modulus. Dynamic deformation modulus always higher than the static deformation. The slope for clastic group is 52-55%, carbonate group is 53-55% and plutonic group is 50%, as shown in Figures 6.5 to 6.13. Figure 6.14 shows a combined plot between the static and dynamic moduli for all tested rocks.

Table 6.3 Parameters for prediction static deformation modulus depending on rock type.

Rock type	X	Y
Phra Wihan sandstone	0.4381	2.5295
Sao Khua sandstone	0.4436	2.2104
Phu Tok sandstone	0.4433	1.4027
Phu Phan sandstone	0.4390	2.5947
Phu Kradung sandstone	0.4350	2.4946
Khao Khad marble	0.4401	1.3619
Khao Khad limestone	0.4392	2.3956
Khao Khad travertine	0.4428	2.4682
Tak granite	0.4411	1.8169

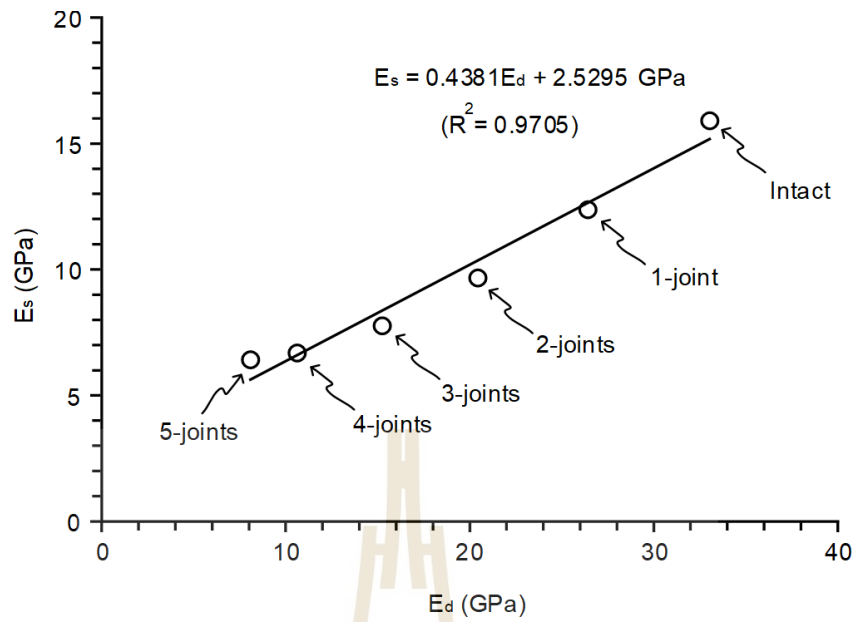


Figure 6.5 Relationship between dynamic and static deformation moduli of Phra Wihan sandstone.

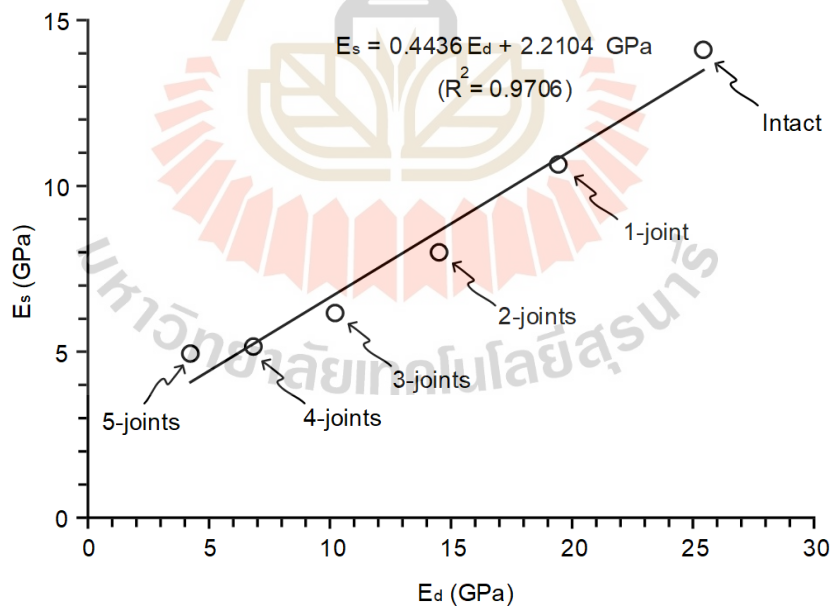


Figure 6.6 Relationship between dynamic and static deformation moduli of Sao Khua sandstone.

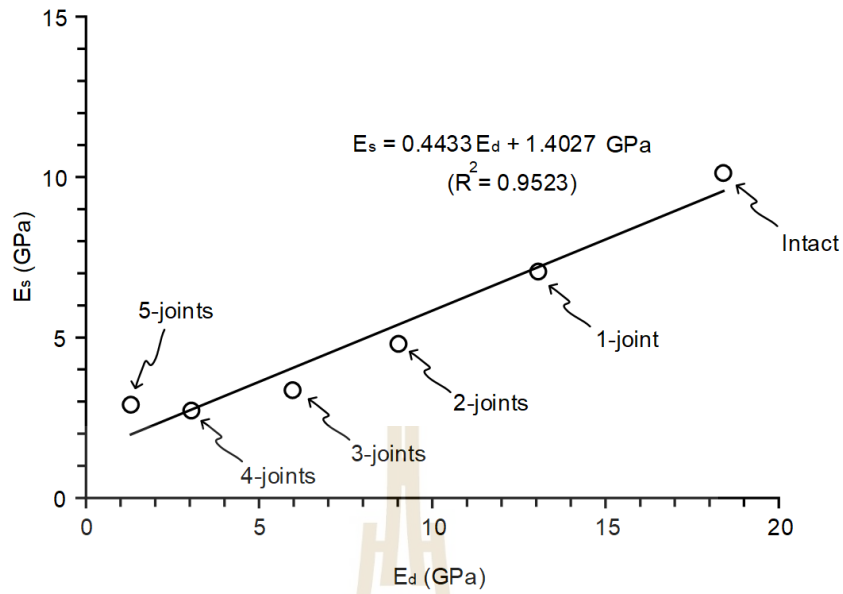


Figure 6.7 Relationship between dynamic and static deformation moduli of Phu Tok sandstone.

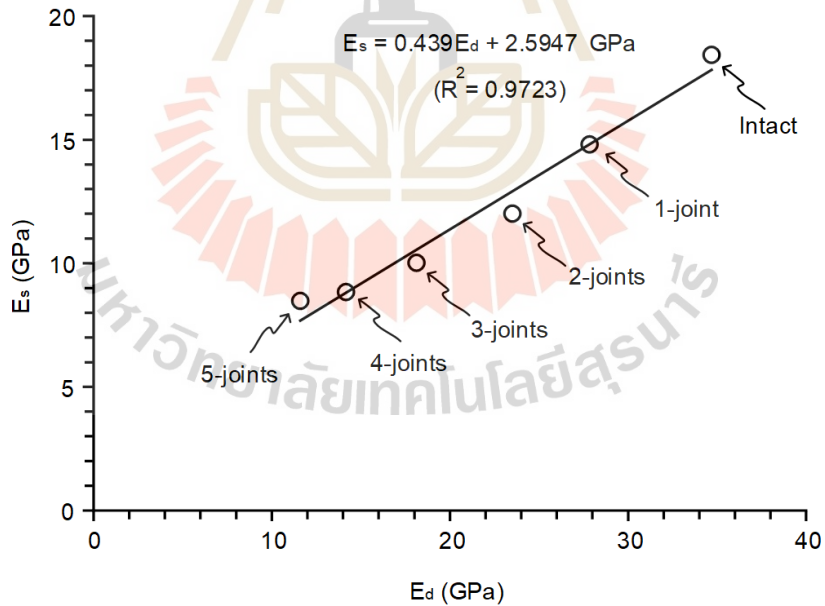


Figure 6.8 Relationship between dynamic and static deformation moduli of Phu Phan sandstone.

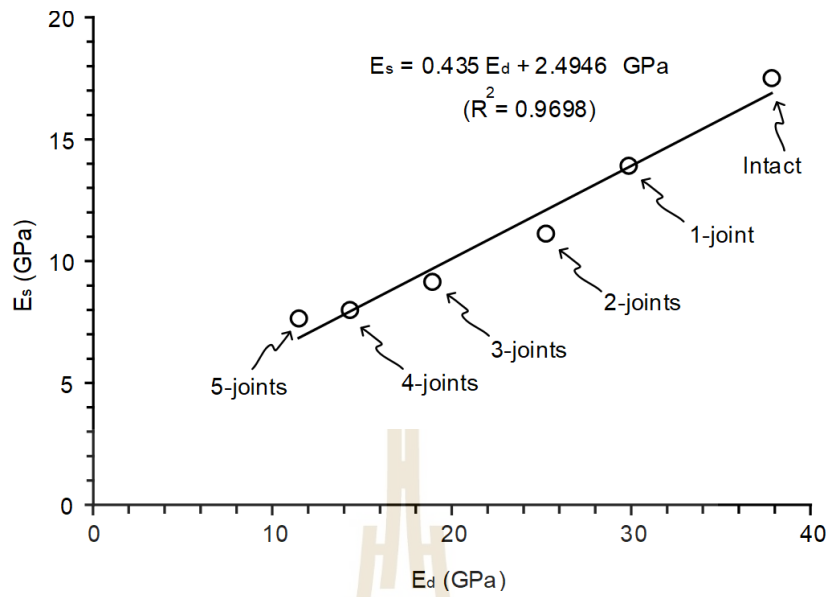


Figure 6.9 Relationship between dynamic and static deformation moduli of Phu Kradung sandstone.

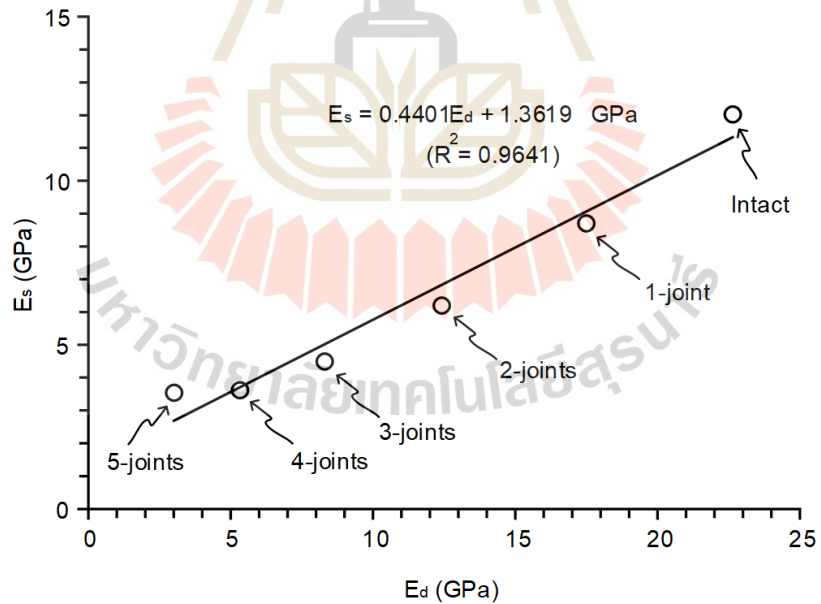


Figure 6.10 Relationship between dynamic and static deformation moduli of Khao Khad marble.

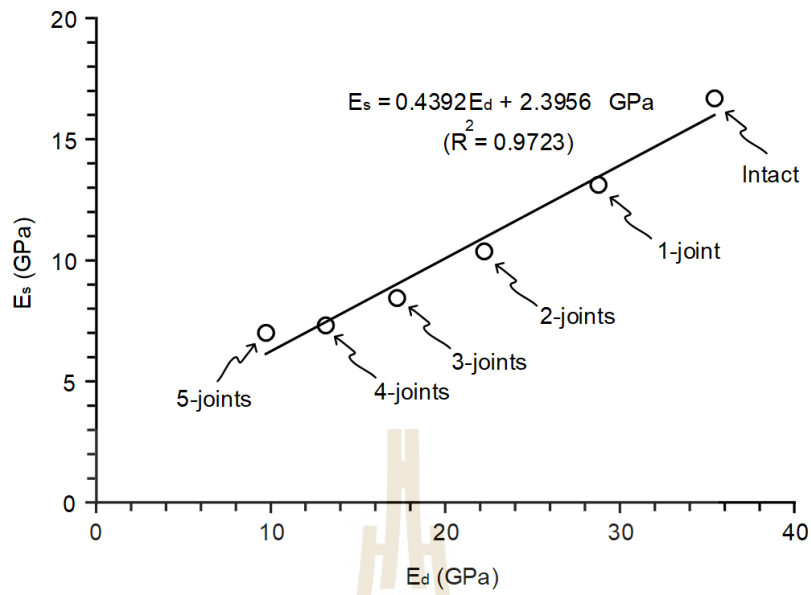


Figure 6.11 Relationship between dynamic and static deformation moduli of Khao Khad limestone.

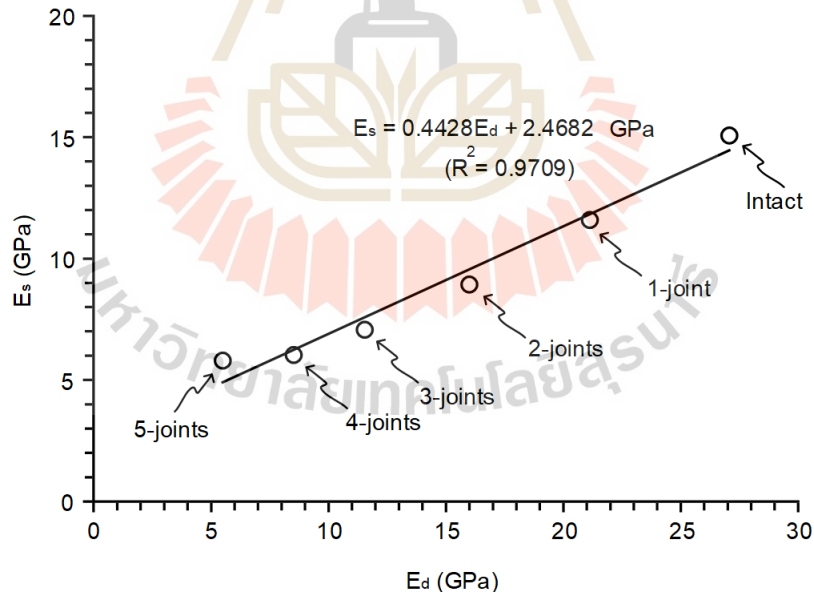


Figure 6.12 Relationship between dynamic and static deformation moduli of Khao Khad travertine.

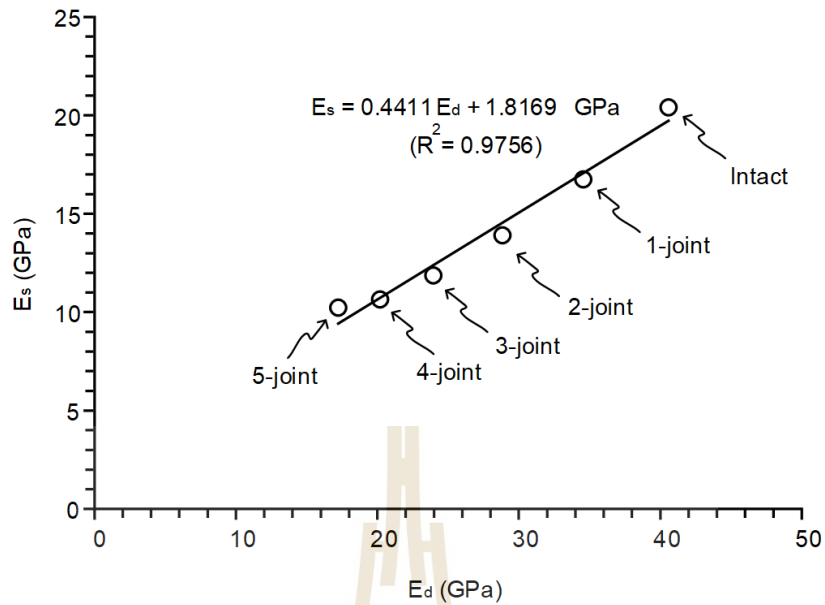


Figure 6.13 Relationship between dynamic and static deformation moduli of Tak granite.

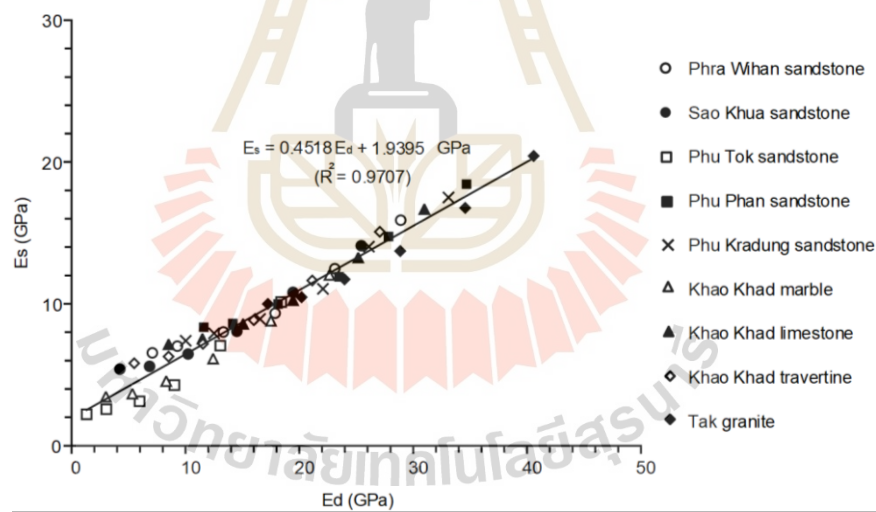


Figure 6.14 Correlation between dynamic and static deformation modulus for all rock types.

6.6 Comparison with previous studies between dynamic and static deformation modulus

Figure 6.15 compares the results from this study (obtained from Figure 6.14) with those obtained from research performed elsewhere. All show linear relations between the static and dynamic moduli. The linear relation between dynamic and static deformation modulus of this study is similar to those of McCann and Entwisle (1992). It is presumed that the different slopes are caused by different rock types which show different stiffness values for the intact condition of the rocks.

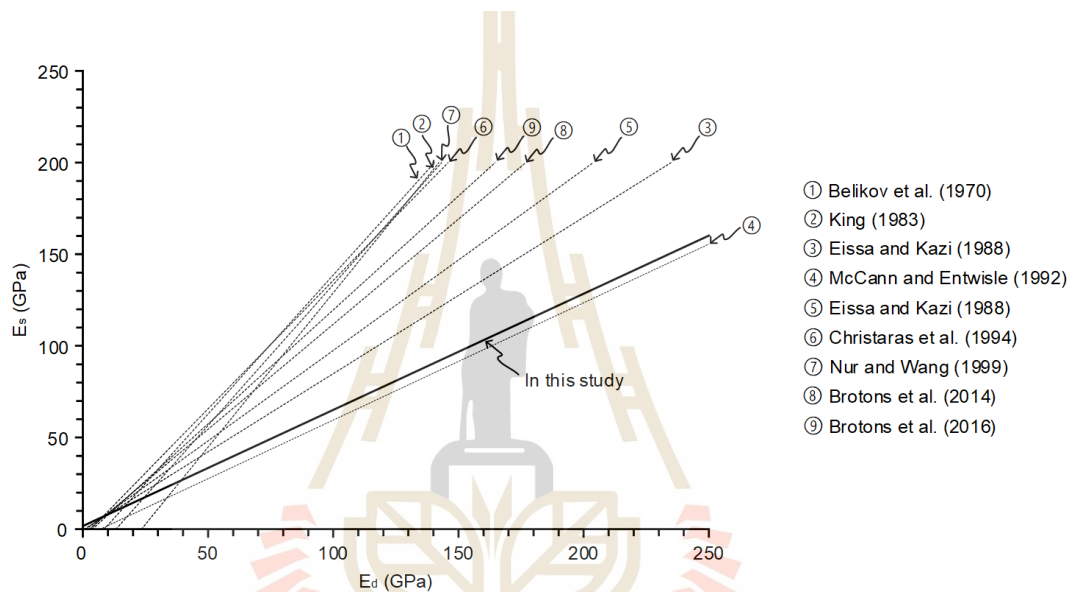


Figure 6.15 Comparison with previous studied between dynamic and static deformation modulus; ① Belikov et al. (1970), ② King (1983), ③ Eissa and Kazi (1988), ④ McCann and Entwisle (1992), ⑤ Eissa and Kazi (1988), ⑥ Christaras et al. (1994), ⑦ Nur and Wang (1999), ⑧ Brotons et al. (2014), and ⑨ Brotons et al. (2016).

CHAPTER VII

DISCUSSIONS AND CONCLUSIONS

7.1 Discussions

The study has focused on the effects of rock fractures on dynamic and static deformation moduli and on the development of their mathematical relationship under a different number of fractures.

The length of rock samples and the number of artificial features are limited by the ultrasonic pulse velocity measurement instrument. The testing is selected on artificial features with roughness induced by tensile stress. This allows measuring the apertures for each fracture that continuously increases from one to five planes. This cannot be accomplished by using artificial saw-cut fracture. The results obtained here agree with those obtained by Watanabe and Sassa (1995), Boadu (2000), Kahraman, (2001). They tend to show that rock fractures are an important fracture for the decreases of wave velocities.

Altindag (2012) and Yasar and Erdogan (2004) describe the wave velocity of rocks which was related to the uniaxial compressive strength (UCS), and Young's modulus (E) for each rock type. Moradian (2009), Yilmaz et al. (2011), Selçuk and Nar (2016), Daoud et al. (2017) predict the uniaxial compressive strength of intact rocks by using ultrasonic pulse velocity. Their test results agree with those of this study that the high wave velocity rocks tend to show high uniaxial compressive strength and Young's modulus.

Measurement of elastic deformation modulus ($E_{m,m}$) is the measurement obtained by averaged tangent of stress-strain curves. Calculation of elastic deformation modulus ($E_{m,c}$) represents the prediction obtained by calculating from equation (2.3) of Thaweeboon et al. (2017) which has been modified from that of Goodman (1970). Joint normal stiffness is varied with Young's Modulus which agrees with the results obtained by Kulatilake et al. (2001). They also agree reasonably well with Starzec (1999) that the dynamic deformation modulus (E_d) is higher than that of the static deformation modulus (E_s).

The relationship between dynamic and static deformation moduli and the number of fractures shows the reduction of parameters by the increase of the numbers of fractures (Figures 6.1 and 6.2). The slope values of dynamic and static deformation modulus are contributed by joint normal stiffness (K_n). The relationship between

dynamic and static deformation moduli have been studied and compiled in many previous researching by Davarpanah et al. (2020). The linear relation of this study shows the same trends with their results (Figure 6.15)

7.2 Conclusions

The induced fractures studied here are normal to the direction of wave propagation during UPV measurements, and to the loading direction of the static tests. Conclusions drawn from this study can be summarized as follows:

1. P and S-wave velocities decrease with increasing number of fractures in rocks.
2. Both static and dynamic Young's moduli decrease with increasing number of fractures.
3. The static and dynamic Young's moduli can be correlated using polynomial equations.
4. The rate change of the E_s -to- E_d ratios tends to be similar for all rocks tested here.
5. For all rock types, E_d for intact rocks is about twice of the E_s . The differences become smaller for rock specimens containing larger number of fractures.

7.3 Recommendations for future studies

The results for the relationship between dynamic and static deformation moduli have been limited to rock samples. To recommendations for more testing is required as follows:

1. The effect of fracture orientation under dry and saturated conditions should be investigated to obtain the results that are close to in-situ condition.
2. More testing and analyses on several rock types would be statistical by enhance reliability of the test results in this study.

REFERENCES

- Altindag, R. (2012). Correlation between P-wave velocity and some mechanical properties for sedimentary rocks. *Journal of the Southern African Institute of Mining and Metallurgy*. 112(3): 229-237.
- ASTM D2845-08. (2008). *Standard Test Method for Laboratory Determination of Pulse Velocities and Ultrasonic Elastic Constants of Rock*. In Annual Book of ASTM Standards. Philadelphia: American Society for Testing and Materials.
- ASTM D7012-14. (2014). *Standard Test Methods for Compressive Strength and Elastic Moduli of Intact Rock Core Specimens under Varying States of Stress and Temperatures*. In Annual Book of ASTM Standards. Philadelphia: American Society for Testing and Materials.
- Boadu, F. K. (2000). Predicting the transport properties of fractured rocks from seismic information: numerical experiments. *Journal of Applied Geophysics*. 44(2-3): 103-113.
- Chamwon, S. (2020). Correlations between ultrasonic pulse velocities and mechanical properties of rocks. *Doctoral dissertation, School of Geotechnology Institute of Engineering Suranaree University of Technology*.
- Daoud, H. S. D., Rashed, K. A. R., and Alshkane, Y. M. A. (2017). Correlations of uniaxial compressive strength and modulus of elasticity with point load strength index, pulse velocity and dry density of limestone and sandstone rocks in Sulaimani Governorate, Kurdistan Region, Iraq. *J Zankoy Sulaimani Part A (Pure Appl Sci)*. 19(3 and 4): 57-72.
- Davarpanah, S. M., Ván, P., and Vásárhelyi, B. (2020). Investigation of the relationship between dynamic and static deformation moduli of rocks. *Geomechanics and Geophysics for Geo-Energy and Geo-Resources*. 6(1): 1-14.
- Fathollahy, M., Uromeiehy, A., and Riahi, M. (2017). Evaluation of P-wave velocity in different joint spacing. *Bollettino di Geofisica Teorica ed Applicata*. 58(3): 157-168.
- Gao, S., Kern, H., Liu, Y. S., Jin, S. Y., Popp, T., Jin, Z. M., and Zhao, Z. B. (2000). Measured and calculated seismic velocities and densities for granulites from xenolith occurrences and adjacent exposed lower crustal sections: A comparative study from the North China craton. *Journal of Geophysical Research: Solid Earth*. 105(B8): 18965-18976.

- Goodman, R.E. (1970). The Deformability of Joints: Determination of the In-Situ Modulus of Deformation of Rock. *ASTM Special Tech. Publ. Philadelphia: American Society for Testing and Materials.*
- Gupta, V., and Sharma, R. (2012). Relationship between textural, petrophysical and mechanical properties of quartzites: a case study from northwestern Himalaya. *Engineering Geology.* 135: 1-9.
- Han, D. H., Nur, A., and Morgan, D. (1986). Effects of porosity and clay content on wave velocities in sandstones. *Geophysics.* 51(11): 2093-2107.
- Hoek, E., and Brown, E. T. (1980). Empirical strength criterion for rock masses. *Journal of Geotechnical and Geoenvironmental Engineering.* 106(ASCE 15715).
- Hoek, E., and Brown, E. T. (1997). Practical estimates of rock mass strength. *International Journal of Rock Mechanics and Mining Sciences.* 34(8): 1165-1186.
- Kahraman, S. (2001). A correlation between P-wave velocity, number of joints and Schmidt hammer rebound number. *International Journal of Rock Mechanics and Mining Sciences.* 38(5):729-733.
- Kahraman, S. (2002). Estimating the direct P-wave velocity value of intact rock from indirect laboratory measurements. *International Journal of Rock Mechanics and Mining Sciences.* 39(1): 101-104.
- Kahraman, S. (2002). The effects of fracture roughness on P-wave velocity. *Engineering Geology.* 63(3-4): 347-350.
- Kahraman, S. (2007). The correlations between the saturated and dry P-wave velocity of rocks. *Ultrasonics.* 46(4): 341-348.
- Kahraman, S., Soylemez, M., and Fener, M. (2008). Determination of fracture depth of rock blocks from P-wave velocity. *Bulletin of Engineering Geology and the Environment.* 67(1): 11-16.
- Khandelwal, M. (2013). Correlating P-wave velocity with the physico-mechanical properties of different rocks. *Pure and Applied Geophysics.* 170(4): 507-514.
- Klimentos, T. (1991). The effects of porosity-permeability-clay content on the velocity of compressional waves. *Geophysics.* 56(12): 1930-1939.
- Kulatilake, P. H. S. W., Malama, B., and Wang, J. (2001). Physical and particle flow modeling of jointed rock block behavior under uniaxial loading. *International Journal of Rock Mechanics and Mining Sciences.* 38(5): 641-657.
- Kurtulus, CE., Bozkurt, A., and Endes, H. (2012). Physical and mechanical properties of serpentinized ultrabasic rocks in NW Turkey. *Pure and applied Geophysics.* 169(7): 1205-1215.
- Mockovčiková, A., and Pandula, B. (2003). Study of the relation between the static and dynamic moduli of rocks. *Metalurgija.* 42(1): 37-39.

- Moradian, Z. A., and Behnia, M. (2009). Predicting the uniaxial compressive strength and static Young's modulus of intact sedimentary rocks using the ultrasonic test. *International Journal of Geomechanics*. 9(1): 14-19.
- Onalo, D., Oloruntobi, O., Adedigba, S., Khan, F., James, L., and Butt, S. (2018). Static Young's modulus model prediction for formation evaluation. *Journal of Petroleum Science and Engineering*. 171: 394-402.
- Prasujan, P. (2020). Effect of weathering on mechanical degradation of sandstones. *Doctoral dissertation, School of Geotechnology Institute of Engineering Suranaree University of Technology*.
- Rahmouni, A., Boulanouar, A., Boukalouch, M., Géraud, Y., Samaouali, A., Harnafi, M., and Sebbani, J. (2013). Prediction of porosity and density of calcarenite rocks from P-wave velocity measurements. *International Journal of Geosciences*. 4(9): 1292-1299.
- Rao, M. V. M. S., Lakshmi, K. P., Sarma, L. P., and Chary, K. B. (2006). Elastic properties of granulite facies rocks of Mahabalipuram, Tamil Nadu, India. *Journal of Earth System Science*. 115(6): 673-683.
- Seephan, K. (2018). Effect of joint frequency and orientation on compressive strength and deformability of small-scale rock mass models. *Doctoral dissertation, School of Geotechnology Institute of Engineering Suranaree University of Technology*.
- Selçuk, L., and Nar, A. (2016). Prediction of uniaxial compressive strength of intact rocks using ultrasonic pulse velocity and rebound-hammer number. *Quarterly Journal of Engineering Geology and Hydrogeology*. 49(1): 67-75.
- Sousa, L. M., del Río, L. M. S., Calleja, L., de Argandona, V. G. R., and Rey, A. R. (2005). Influence of microfractures and porosity on the physico-mechanical properties and weathering of ornamental granites. *Engineering Geology*. 77(1-2): 153-168.
- Starzec, P. (1999). Dynamic elastic properties of crystalline rocks from south-west Sweden. *International Journal of Rock Mechanics and Mining Sciences*. 36(2): 265-272.
- Thaweeboon, S., Dasri, R., Sartkaew, S., and Fuenkajorn, K. (2017). Strength and deformability of small-scale rock mass models under large confinements. *Bulletin of Engineering Geology and the Environment*. 76(3): 1129-1141.
- Tuğrul, A., and Zarif, I. H. (1999). Correlation of mineralogical and textural characteristics with engineering properties of selected granitic rocks from Turkey. *Engineering geology*. 51(4): 303-317.

- Vanorio, T., Prasad, M., and Nur, A. (2003). Elastic properties of dry clay mineral aggregates, suspensions and sandstones. *Geophysical Journal International*. 155(1): 319-326.
- Watanabe, T., and Sassa, K. (1995, June). Velocity and amplitude of P-waves transmitted through fractured zones composed of multiple thin low-velocity layers. *International Journal of Rock Mechanics and Mining Sciences & Geomechanics Abstracts*. 32(4): 313-324.
- Yagiz, S. (2011). P-wave velocity test for assessment of geotechnical properties of some rock materials. *Bulletin of Materials Science*. 34(4): 947.
- Yasar, E., and Erdogan, Y. (2004). Correlating sound velocity with the density, compressive strength and Young's modulus of carbonate rocks. *International Journal of Rock Mechanics and Mining Sciences*. 41(5): 871-875.
- Yilmaz, N. G., Goktan, R. M., and Kibici, Y. (2011). Relations between some quantitative petrographic characteristics and mechanical strength properties of granitic building stones. *International Journal of Rock Mechanics and Mining Sciences*. 48(3): 506-513.



BIOGRAPHY

Ms. Krittiyaporn Singkraihaan was born on May 8, 1996 in Nongkhai Province, Thailand. She received her Bachelor's degree in Engineering (Geological Engineering) from Suranaree University of Technology in 2019. For her post-graduate, she continued to study with a Master's degree in the Geological Engineering Program, Institute of Engineering, Suranaree university of Technology.

